

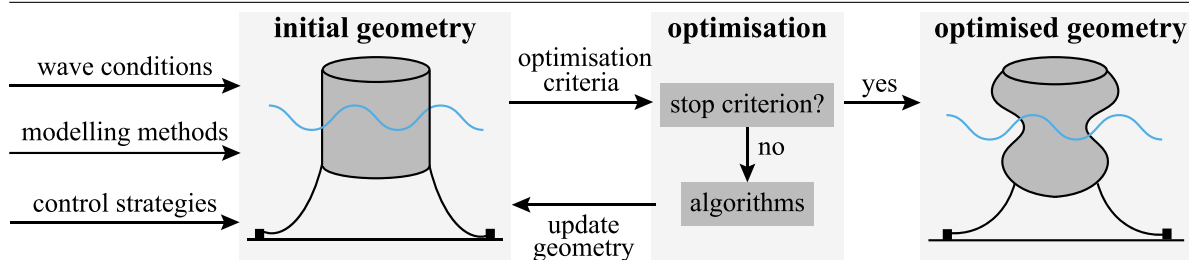
# Geometric optimisation of wave energy conversion devices: A survey<sup>☆</sup>

Bingyong Guo<sup>a,b</sup>, John V. Ringwood<sup>b,\*</sup>

<sup>a</sup> School of Marine Science and Technology, Northwestern Polytechnical University, Xi'an, Shaanxi 710072, China

<sup>b</sup> Centre for Ocean Energy Research, Maynooth University, Maynooth, Co. Kildare, Ireland

## GRAPHICAL ABSTRACT



## ARTICLE INFO

### Keywords:

Wave energy conversion  
Geometric optimisation  
Optimisation algorithm  
Optimisation criteria  
Optimal control  
Hydrodynamic modelling

## ABSTRACT

Unlike more established renewable energy conversion technologies, such as wind turbines, wave power systems have reached neither commercial maturity, nor technological convergence. The significant variation in device geometries and operating principles has resulted in a diversification of effort, with little coordination or true comparative analysis. The situation is compounded by the relative lack of systematic optimisation applied to the sector, partly explained by the complexity and uncertainty associated with wave energy system models, as well as difficulties in the evaluation of appropriate target function metrics. This review provides a critical overview of the state-of-the-art in wave energy device geometry optimisation, comparing and contrasting various optimisation approaches, and attempting to detail the current limitations preventing further progress, and convergence, in the development of optimal wave energy technology.

## 1. Introduction

The concept to utilise ocean waves to generate useful energy is not new, and the first patent dates back to 1799 [1], with more than 1000 wave energy conversion patents registered by 1980 [2]. Due to the fossil fuel crisis in the 1970s, research and development activities to harvest energy from ocean waves were boosted dramatically, inspired by the enormous wave power potential, estimated at  $2.11 \pm 0.05$  TW globally [3]. Over the past two decades, remarkable progress has been made to improve the technology performance level (TPL) [4] and technology readiness level (TRL) of wave energy converters (WECs), by

applying novel modelling methods and control strategies [5–12], developing novel power take-off (PTO) mechanisms [13–19], and conducting sea trials [20–26]. However, wave energy is still virtually untapped and large scale commercial application of wave energy conversion technology is mainly hindered by the associated high levelised cost of energy (LCoE). The LCoE of wave energy ranges from 90 €/MWh to 490 €/MWh, which is higher than that of fossil fuels and other renewable resources [27], e.g. wind energy.

A WEC device converts the kinetic and/or potential energy contained in moving waves to useful energy (mainly electricity), comprising floating or submerged bodies, PTO units, control systems, power

<sup>☆</sup> This document is the result of a research project funded by the Marie Skłodowska-Curie Action (Grant No. 841388) and Science Foundation Ireland (Grant No. SFI/13/IA/1886).

\* Corresponding author.

E-mail addresses: [bingyong.guo@mu.ie](mailto:bingyong.guo@mu.ie) (B. Guo), [John.Ringwood@mu.ie](mailto:John.Ringwood@mu.ie) (J.V. Ringwood).

URLs: <https://coer.maynoothuniversity.ie/members/bingyong-guo/> (B. Guo), <https://ee.maynoothuniversity.ie/jringwood/> (J.V. Ringwood).

<https://doi.org/10.1016/j.apenergy.2021.117100>

Received 25 November 2020; Received in revised form 4 May 2021; Accepted 18 May 2021

0306-2619/© 2021 The Authors. Published by Elsevier Ltd. This is an open access article under the CC BY-NC-ND license

(<http://creativecommons.org/licenses/by-nc-nd/4.0/>).

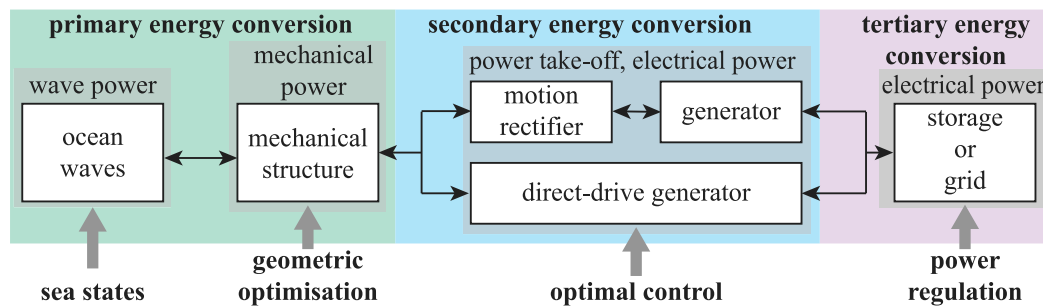


Fig. 1. The complete wave-to-wire energy conversion train of a wave energy conversion device.

electronics and other accessories. In general, the energy transfer chain in a WEC device can be divided into three stages, as shown in Fig. 1, including primary, secondary, and tertiary, energy conversion stages. At the primary energy conversion stage, wave power is converted to mechanical power by the wave–structure interaction (WSI) between ocean waves and structures/bodies. At this stage, geometric optimisation is required to improve the hydrodynamic performance of WSI for the specific wave conditions of the installation site, which can be represented by (somewhat ideal) regular waves, irregular waves or wave climates. In addition, some novel WEC concepts utilise adaptable structures and adjust the shape of the structure according to incident waves to influence the WSI process [28–30], which results in even more complicated geometric optimisation problem. As mechanical structures are coupled with PTO systems, e.g. generators, the secondary energy conversion stage transfers mechanical power into electrical power. The coupling can be direct, e.g. via a direct-drive generator, or indirect, where the structure’s motion is, for example transferred to rotational motion by air turbines [18], hydraulic rams [23], gearboxes [31] or mechanical motion rectifiers [32]. At this stage, optimal control strategies are useful to tune the system dynamics to maximise power output [9,12]. For WECs that oscillate, end-stop protection is required and can be achieved by control [9,33] or mechanical design [34,35]. In general, the generated electrical power is of low quality, characterised by a non-standard alternating-current (AC) profile. Hence, the tertiary energy conversion stage, utilising power electronics to improve power quality, is used to transfer the non-standard AC power into direct-current (DC) power for energy storage or standard AC power for grid integration [14,36]. Noting that the power flow between these stages can be either unidirectional or bidirectional, mainly depending upon PTO systems and control strategies.

For successful large-scale commercial application, it is recommended to evaluate the TPL and TRL at early stage, and development trajectories prioritising the TPL over TRL are likely to require much less development time and cost [4,37]. To evaluate the TPL of a WEC concept, economic life-cycle performance evaluation is needed and design optimisation is of critical importance to improve the TPL [38]. In addition, optimised WEC hull geometry also contributes to improving system reliability [39]. For a generic WEC device, containing the aforementioned three energy conversion stages (see Fig. 1), design optimisation, i.e. geometric optimisation and optimal control, is required at the primary and secondary stages, respectively. There are several reviews summarising control strategies for power maximisation of WEC systems, including [9–12]. However, to date, a comprehensive review of geometric optimisation of WEC devices is still missing, and the aim of this study is to survey geometric optimisation approaches to improve the hydrodynamic performance of WEC systems at the primary stage. This paper focuses on the geometric optimisation of various stand-alone WEC devices rather than WEC array layout optimisation, which is covered in [40–50].

The WEC geometric optimisation process is illustrated in Fig. 2. For an initial WEC device concept, the first step is to define the structure and its modes to harvest wave energy via WSI. Based on design wave

conditions and the corresponding WSI performance, a scaled-down experimental model or a numerical model can be determined to evaluate the device dynamics and performance. To obtain more practical results, control force and some critical nonlinear factors should be taken into account at this step, as energy-maximisation control approaches tend to exaggerate the WEC motion and non-linearities [51,52]. Therefore, the optimised geometry varies when control methods change [33,53]. For instance, the optimised radii of semi-submersed cylindrical heaving point absorbers are 14 m and 6 m for passive control and latching control [53], respectively. After evaluating the device motion and performance, optimisation algorithms can be used to update the geometric parameters, and the procedure goes back to the first step, repeating all the aforementioned steps until the system performance is maximised.

As shown in the flowchart in Fig. 2, the optimised geometry depends on WEC concept, geometric shape, design wave conditions, WSI modelling methods, control strategy employed, performance criteria and the optimisation algorithm employed. The influence of each of these factors on WEC geometric optimisation will be discussed in detail in this survey. Mooring design may also affect the performance of some specific devices when wave direction is taken into account [54], but is not considered in this study as a generic factor. In this paper, the focus will be WEC geometry optimisation through device simulation. While adapting and evaluating *physical* models in an experimental setting is also an option, the costs associated with such an activity are excessive, and the number of design iterations are limited. Nevertheless, rough, small-scale, physical model evolution can play a useful role in the improvement of basic WEC concepts.

The remainder of the paper is organised as follows: Section 2 investigates various concepts of wave energy conversion and their associated generic geometric shapes, while Section 3 considers design wave conditions for WEC hydrodynamic optimisation, including regular and irregular waves, and wave climates. Section 4 summarises hydrodynamic modelling approaches to represent WSI in both numerical and physical domains, with Section 5 examining the importance of PTO model fidelity on WEC geometry optimisation. Section 6 discusses model simplification possibilities and the implementation of WSI and PTO modelling for WEC geometric optimisation. Energy-maximisation control strategies, and their effect on WEC geometric optimisation, are considered in Section 7. In Sections 8 and 9, the foci are optimisation criteria and algorithms, respectively. Section 10 gives an overview of the usage rates of various WEC concepts, wave conditions, modelling methods, control strategies, performance criteria and optimisation algorithms. Comprehensive discussion on the aforementioned factors are detailed in this section, together with some recommendations for conducting WEC geometric optimisation. Finally, Section 11 draws some conclusions on how these aforementioned factors influence the optimised WEC geometry.

## 2. Wave energy converters

Since wave energy conversion concepts diverge, with over 1000 devices reported [2], there is no unique categorisation method to cover

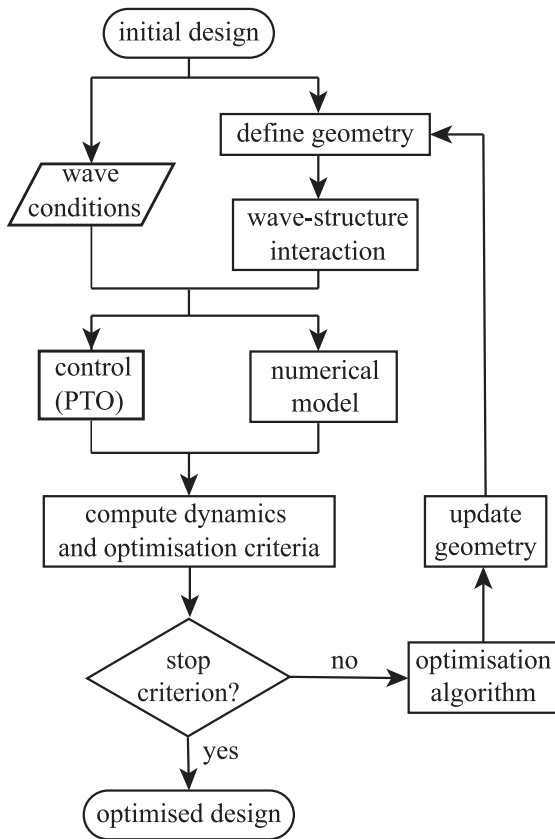


Fig. 2. Flowchart of geometric optimisation for a generic wave energy conversion device.

all kinds of WEC systems. In general, WEC systems can be classified according to their deployment locations, working principles, operation modes and device geometries [8,55–57]. This section gives an overview of WEC shapes of four primary types, i.e. point absorbers (PAs), oscillating wave columns (OWCs), attenuator-type WECs (AWECs) and terminator-type WECs (TWECS). Noting that this classification is mainly based on device geometry and working principle, providing different basic starting points for device optimisation. In this section, working principles, operation modes and geometric shapes of each type will be introduced.

2.1. Point absorbers

Point absorbers are referred to the WEC devices whose characteristic dimensions are much smaller than the incident wave length. PAs may operate in heave, pitch or multiple degrees of freedom (DoFs), and situate nearshore or offshore. From the body geometry viewpoint, PAs can be classified into two sub-types, including one-body PAs and two-body PAs. The former are generally referenced to the sea bed or offshore structures, with an absolute displacement reference, while the latter are mainly self-referenced. Typical hull shapes of one-body and two-body PAs are summarised in Tables 1 and 2, respectively.

One-body PAs utilise one floating or submerging body to interact with ocean waves, and the body’s motion is referenced to a fixed PTO device to generate electricity. The body dynamics has low-pass characteristics in the frequency domain, and the natural frequency and response amplitude operator (RAO) depends significantly on the geometric shape of the body. When the natural resonant frequency is distant from the wave frequency, control strategies can be used to tune the device’s natural frequency towards wave frequency for power maximisation [9–12,58]. Table 1 summarises 9 fundamental geometric

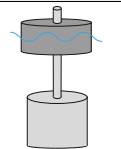
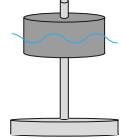
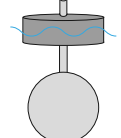
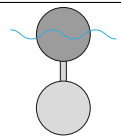
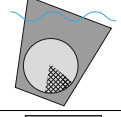
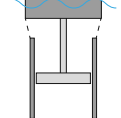
Table 1 Typical geometric shapes for one-body point absorbers.

Schematic	Shape	Parameters	References
	Cylinder (Cyl)	Radius Height Draught	[33,39,48,53,63–79]
	Cylinder-moonpool (CylMpl)	Radii Height Draught	[68]
	Cone (Con)	Radius Cone Angle Draught	[65,77,80,81]
	Cylinder-cone (CylCon)	Radius Heights Cone Angle Draught	[67,72,73,76,82–87]
	Cone-Cylinder-cone (ConCylCon)	Radius Heights Cone Angle Draught	[78]
	Sphere (Sph)	Radius Draught	[39,65,73,78]
	Cylinder-sphere (CylSph)	Radius Height Draught	[67,72,73,76,83,85,87–89]
	Cuboid (Cub)	Length Width Height Draught	[39,90,91]
	Arbitrary shape (ArbShp)	Points draught freeboard	[59–62,92–95]

shapes for one-body PAs, including: (i) cylinder (Cyl), (ii) cylinder with moonpool (CylMpl), (iii) cone (Con), (iv) cylinder-cone (CylCon), (v) cone-cylinder-cone (ConCylCon), (vi) sphere (Sph), (vii) cylinder-sphere (CylSph), (viii) cuboid (Cub), and (ix) arbitrary shape (ArbShp). Geometric parameters of the hull shapes vary from case to case, but should define the hull’s length, width, draught and freeboard. For the cylinder-cone and cone-cylinder-cone shapes, the red dashed lines illustrate that the cones can be truncated to form frustums. For the hull shape marked of arbitrary shape, the geometry is flexibly defined by control points [59–62].

The hull of one-body PAs can be either floating, e.g. the Seabased Buoy [68], or fully submerged, e.g. the CETO buoy [66]. A floating PA device usually comprises a symmetrical structure floating on the sea surface and a PTO system fixed to the sea bed. Hence, the floater’s draught has a significant influence on its hydrodynamics. For fully submerged devices, the submergence depth becomes an important factor that should be taken into account in geometric optimisation, as it significantly affects a PA’s hydrodynamic performance [78]. One-body PAs mainly operate in heave mode and are largely insensitive to wave direction. Hence, most of these shapes are axisymmetric. When wave direction is taken into account in the geometric optimisation procedure, the optimised profile may diverge from an axisymmetric shape. For instance, the optimised profile for a submerged planar pressure differential WEC depends significantly on wave direction [62]. Only when the wave direction is evenly distributed in  $[0, 2\pi]$ , a circular horizontal section is obtained via geometric optimisation [62]. In addition, 10 shapes of a one-body heaving PA are compared in [87], to increase hydrodynamic efficiency by modifying the bottom shape.

**Table 2**  
Typical geometric shapes for two-body point absorbers.

Schematic	Shape	Parameters	References
	Cylinder–cylinder (Cyl–Cyl)	Radii Height Draught	[97–100]
	Cylinder–plate (Cyl–Plt)	Radii Draught	[97,99,101]
	Cylinder–sphere (Cyl–Sph)	Radii Height Draught Submergence	[99,100]
	Sphere–sphere (Sph–Sph)	Radii Draught Submergence	[102]
	Hull–pendulum (Hul–Pdl)	Profile Draught	[96,103–106]
	Cylinder–piston (Cyl–Pst)	Radii Height Draught Submergence	[107]

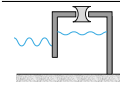
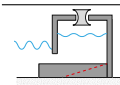
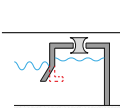
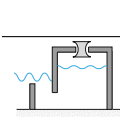
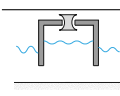
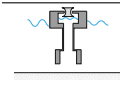
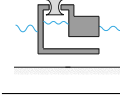
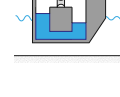
Two-body point absorbers exploit the relative motion between two bodies. Since two-body PAs are not attached to a fixed reference, mooring systems are indispensable, and two-body PAs are suitable for the offshore environment. In contrast to one-body PAs, two-body PAs have band-pass characteristics, with flexibility to tune the passband to certain wave spectra [34,35]. Table 2 details 6 typical geometric shapes for two-body PAs, including: (i) cylinder–cylinder (Cyl–Cyl), (ii) cylinder–plate (Cyl–Plt), (iii) cylinder–sphere (Cyl–Sph), (iv) sphere–sphere (Sph–Sph), (v) hull–pendulum (Hul–Pdl), and (vi) cylinder–piston (Cyl–Pst). In this study, the ‘plate’ shape consists of a cylinder with a relatively small height with respect to its diameter. The hull–pendulum structure is a self-contained pitching WEC, and only the external structure interacts with waves, e.g. the SEAREV device [96]. The others mainly operate in heave with axisymmetric shapes.

Compared to one-body PAs, the geometric shapes of two-body PAs are more complex, and more parameters are used to define their geometries. While one-body PAs are characterised by low-pass characteristics, two-body PAs perform as band-pass filters, with the respective bandwidth depending significantly on the geometric shapes. Most PAs are oscillatory and, hence, end-stop protection is required. Only a few two-body PAs, e.g. the SEAREV [96,104], utilise rotational pitching motion for energy harvesting, avoiding the need for end-stop protection. In addition, comparison studies of the Cyl–Cyl and Cyl–Plt shapes are discussed in [97,99].

## 2.2. Oscillating water columns

An oscillating water column device utilises a hollow structure with an open inlet below the still water level to trap air in its chamber above the inner free-surface; wave action alternately compresses and

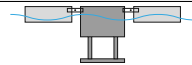
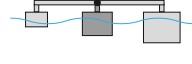
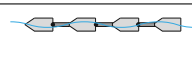
**Table 3**  
Typical geometric shapes for oscillating water columns.

Schematic	Shape	Parameters	References
	Universal fixed (UnivFix)	Chamber size Orifice size Submergence	[108–111]
	Bottom-shaped (BtmShp)	Chamber size Orifice size Submergence Bottom shape	[112–115]
	Front-shaped (FrntShp)	Chamber size Orifice size Submergence Front wall	[116,117]
	U-shape	Chamber size Orifice size Submergence	[118,119]
	Universal floating (UnivFlt)	Chamber size Orifice size Draught	[120–123]
	Spar-buoy	Chamber size Orifice size Draught	[124–126]
	Backward bent duct buoy (BBDB)	Height Length Width	[127]
	UGEN	Radii Height Draught Submergence	[128]

decompresses the trapped air, which forces air to flow through a turbine coupled to a generator [18]. Since there is no oscillating linear motion in OWCs, end-stop function is not required. In general, OWCs can be either fixed or floating, with fixed OWCs attached to coasts or breakwaters [108,109]. Table 3 summarises 8 typical geometric shapes of OWCs, with the first four fixed, with the latter 4 floating, with the red dashed lines giving alternative geometric shapes of fixed OWCs. One great advantage of fixed OWCs is that the cost of infrastructure can be shared by other functional requirements, e.g. breakwaters [109], and, hence, it is possible to reduce the LCoE to a lower level. In addition, open sea trials of fixed OWCs validate their reliability and survivability in extreme sea states [20].

For fixed OWCs, four typical geometric shapes are illustrated in Table 3, including universal fixed (UnivFix), bottom-shaped (BtmShp), front-shaped (FrntShp) and U-shape OWCs. OWC geometric optimisation mainly focuses on the chamber shape, orifice size and structure submergence. Properly designed shapes of front wall or/and bottom can increase the hydrodynamic performance of fixed OWCs [112,113,116]. The geometric optimisation of U-shape OWCs mainly focuses on the shapes and geometric parameters of the U-shape duct [118,119]. In addition, four typical geometric structures of floating OWCs are shown in Table 3, including universal floating (UnivFlt), spar-buoy, backward bent duct buoy (BBDB), and UGEN (floating device with a U tank for Generation of electricity from waves) OWCs. The corresponding geometric parameters for optimisation are chamber shape, orifice size and device draught. Notably, the orifice is treated as an ideal and simple PTO alternative. In addition, a variety of bottom shapes of an OWC device was compared in [113], concluding that a circular curved bottom profile performs better than triangular or stepped bottom profiles.

**Table 4**  
Geometric shapes for attenuator-type wave energy converters.

Schematic	Shape	Parameters	References
	Barge	Number Length	[130,131]
	M4	Radii Distance Submergence	[129]
	Seaweed	Length Draught Distance	[132]

### 2.3. Attenuators

Attenuators are floating WEC devices oriented parallel to the wave direction, usually composed of multiple floating bodies connected by hinged joints, with the relative motion between two connected bodies used to generate electricity via PTO devices. The notable attenuator-type WECs are the Pelamis [23], using multiple semi-submerged cylindrical sections, the M4 device [129], using multiple cylindrical buoys, and the McCabe Wave Pump hinged barge device [130,131], using floating cuboid rafts. Table 4 shows the geometric shapes of the barge-like, M4-like, and Pelamis-like attenuators. For barge-like devices, the number of barges and the length of each barge should be optimised to improve hydrodynamic performance. For the other two subtypes of attenuators, the length and draught of each segment, and the distance between two connected segments should be optimised. These AWECs mainly oscillate in pitch and, hence, end-stop function is required. In addition, a comparison study is conducted experimentally in [129] to investigate the influence of scale and bottom shape on the capture width ratio (CWR) of the M4 device.

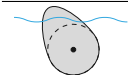
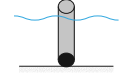
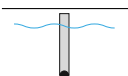
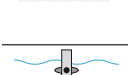
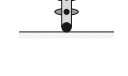
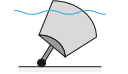
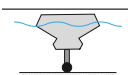
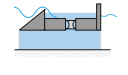
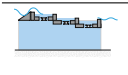
### 2.4. Terminators

Terminators are oriented perpendicular to the wave direction, typically including duck-like devices, oscillating wave surge converters (OWSCs) and overtopping devices. Table 5 summarises 9 typical geometric shapes, one for duck-like devices, five for OWSCs and three for overtopping devices. For duck-like devices, the parameters of submergence and beak angle are optimised [133]. OWSCs utilise various geometric shapes for WSI, including cylinders, flaps, flaps with vanes, C-cell shape and arbitrary-shape flaps. For these shapes, the flap size and submergence are the most important design parameters. Notably, cylinder-shaped devices (the second shape in Table 5) can be classified as PAs, but treated as OWSCs here as their working principle and optimisation method are closer to other OWSCs. The vane angle of the flap-vane OWSCs can be controlled in real time to achieve a constant power output [28], which shows great potential in large-scale commercial applications. Overtopping devices are exemplified by the wave dragon (WD) device [134–137], the WaveCat device [138–140] and the sea slot-cone generator (SSG) device [141–144], for which the angle, freeboard and draught, and ramp shape, are the main geometric parameters for optimisation. For SSG devices, experimental studies also show that optimised wave-focusing walls also contribute to improving SSG performance, in terms of overtopping flow rate [141].

### 2.5. Influence of wave energy converter concept on optimal geometry

The operational modes of wave energy converters have a significant influence on geometric optimisation, since they determine WSI directly. Under a variety of performance metrics, the optimised hull for surge motion will differ dramatically from its counterpart for the modes of surge, heave and pitch [93,95]. In addition, the optimised WEC geometry in surge mode [152] is totally different from its counterpart in

**Table 5**  
Typical geometric shapes for terminator-type wave energy converters.

Schematic	Shape	Parameters	References
	Duck	Submergence Beak angle	[133]
	Cylinder	Radius Height Submergence	[145,146]
	Flap	Length Width Height Submergence	[147–149]
	Flap-vane	Flap size Vane size Vane number Submergence	[28–30]
	C-cell	C-cell profile Height Submergence	[147,150]
	Arbitrary shape (ArbShp)	Control points	[151,152]
	Wave dragon (WD)	Ramp angle Freeboard Submergence	[134–137]
	Catamaran-like WaveCat	Wedge angle Freeboard Draught	[138–140]
	Sea slot-cone generator (SSG)	Crest level Ramp angle Ramp draught	[141–144]

surge and pitch modes [92,94,153]. To maximise the power absorption of a box-hull WEC concept, the box-hull tends to have a large width but a small draught to operate in heave, but tends to have a small width but a large draught in pitch mode [154]. In addition, better performing devices have relatively exaggerated geometry: either a long attenuator-type device or a wide terminator-type device, with dominant contribution from pitch or heave modes, respectively [154].

Even for the same operational mode, WEC performance varies as the hull shape changes. Taking a heaving point absorber as an example, a cylinder with conic bottom outperforms a truncated cylinder in terms of RAO, power absorption and CWR [67,76]. Five hull shapes of heaving PAs are compared in [73], which concludes that the optimised buoy radius depends heavily on the specific shape. In addition, a comparison study of 10 PA shapes in [87] addresses the importance of increasing hydrodynamic efficiency by modifying the bottom shape.

WEC hull shape can be defined by common geometric shapes, e.g. sphere, cylinder, cone etc, or by flexible control points to form arbitrary shape, e.g. Bezier curves [60], the bicubic B-spline surfaces [151, 152], etc. The former method only has a few parameters to be optimised and results in simple structures to ease their manufacturing procedure, while the latter method can lead to streamlined shapes but may increase computational cost due to a large number of control points and manufacturing cost due to a more complex geometry. Additionally, the optimised geometry may also be sensitive to the definition of control points and curves [151].

Tables 1–5 illustrate a wide range of WEC shapes for geometric optimisation. However, as wave energy conversion concepts diverge [2], there are still some WEC geometries, especially some novel concepts, which are hard to fit into the aforementioned classes and tables, e.g. geometric optimisation of the CECO device [155]. In summary, WEC



operation modes and shape definitions, representing the ‘S (structure)’ of WSI, have a significant influence on the optimised geometry, but there is no current concept or shape which outperforms all other concepts or shapes in all cases, which explains the current lack of convergence to an archtypical shape.

### 3. Wave conditions

As shown in Fig. 2, wave conditions, representing the ‘W (wave)’ of WSI, are input data for WEC hydrodynamic optimisation and can significantly affect the optimised WEC dynamics and performance. Therefore, it is very important to define the appropriate design wave conditions before the optimisation procedure. Design wave conditions can be represented by (i) regular waves, (ii) irregular waves described by wave spectra, or (iii) wave climates described by statistical scatter tables or diagrams. This section gives an overview of wave conditions and their influence on WEC geometric optimisation.

#### 3.1. Regular waves

At the initial stage of a WEC concept, simple wave conditions, typically regular waves or harmonic waves, are preferred to obtain some initial impression of WEC dynamics, also giving information about the device dynamics at specific frequencies. Based on linear wave theory, where the wave height  $H$  is much smaller than the wavelength  $\lambda$ , a harmonic wave, at a position  $(x, y)$  and a time instant  $t$ , can be written by

$$\eta(x, y, t) = \frac{H}{2} \cos(\omega t - kx \cos \beta - ky \sin \beta + \varphi), \quad (1)$$

where  $\eta$ ,  $\omega = 2\pi/T$ ,  $T$ ,  $k = 2\pi/\lambda$ ,  $\beta$  and  $\varphi$  are wave elevation, angular frequency, period, wave number, incident angle and initial phase, respectively. For deep water, the wave power per unit width of the wave front,  $J_r$ , also called wave-energy flux, can be defined as

$$J_r = \frac{\rho g^2}{32\pi} T H^2, \quad (2)$$

where  $g$  is the gravity constant.

Regular waves are simple and computationally efficient for WEC geometric optimisation. However, only simple performance criteria, e.g. average power and RAO, can be evaluated, and the resulting in “optimal” geometry may be suboptimal for real ocean waves. Irregular waves should be used for more realistic evaluation of WEC performance. When the wave steepness  $H/\lambda$  is relatively large, linear wave theory may become invalid and the wave elevation can be represented by high-order Stokes wave [2]. For instance, second order Stokes waves are used to optimise the geometry of OWCs in [114,116].

#### 3.2. Irregular waves

Irregular waves can be approximated by a summation of sinusoidal waves. The frequency and amplitude of each component can be determined from wave spectra with its initial phase evenly distributed in  $[0, 2\pi]$ . Among a variety of wave spectra [156], the notable ones are the Pierson–Moskowitz (PM) [157] and the JOint North Sea WAve Project (JONSWAP) spectra [158]. The PM spectrum,  $S(\omega)$ , is generally used to describe fully developed wind waves, given as

$$S(\omega) = \frac{5H_s^2 \omega_p^4}{16 \omega^5} \exp\left(-\frac{5\omega_p^4}{4\omega^4}\right), \quad (3)$$

where  $H_s$ ,  $\omega_p = \frac{2\pi}{T_p}$  and  $T_p$  are the significant wave height, peak angular frequency and peak period, respectively.

In practice, wave spectra can be estimated statistically from wave observation. Hence, the significant wave height and energy period,  $T_e$ , of a given spectrum can be written as

$$H_s = 4\sqrt{m_0}, \quad (4)$$

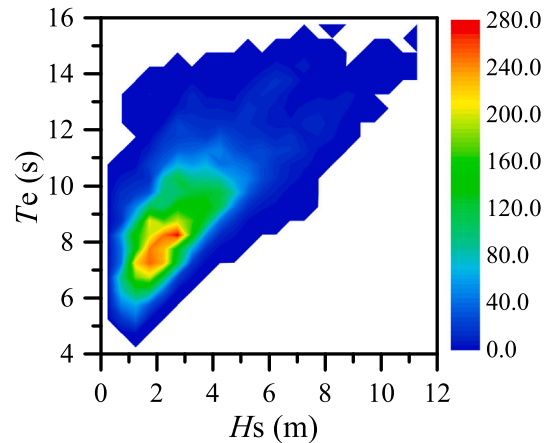


Fig. 3. Wave climate at the Atlantic Marine Energy Test Site.

$$T_e = \frac{m_{-1}}{m_0}, \quad (5)$$

where  $m_i$  is the  $i$ th moment of the spectrum, given as

$$m_i = \int_0^\infty \omega^i S(\omega) d\omega. \quad (6)$$

Therefore, the wave-energy flux for irregular waves,  $J_{ir}$ , can be rewritten as

$$J_{ir} = \frac{\rho g^2}{64\pi} T_e H_s^2. \quad (7)$$

To make the wave-energy flux of irregular waves identical to regular waves, the equivalences  $H = H_s/\sqrt{2}$  and  $T = T_e$  are used.

For a given wave spectrum, wave elevation in the time domain can be realised by randomising wave amplitudes or phases [159]. The pros and cons of these two methods are compared in [159], and their validity depends on the modelling objectives. Compared to regular waves, the use of irregular waves results in more realistic optimised WEC geometry. However, the full variation in sea state (corresponding to the wave climate) at an installation site should be used for WEC hydrodynamic optimisation.

#### 3.3. Wave climate

To evaluate the power performance of WEC systems for a given installation site, annual wave observation statistical data are required, specifying the wave climate, which is generally illustrated by a scatter table or diagram. An example is given in Fig. 3, of which the data are collected at the Atlantic Marine Energy Test Site (AMETS) by the Belmullet Inner (Berth B) wave buoy in 2017 [160]. In this figure, the total occurrence, in hours, of each sea state is presented, and the data availability is as high as 8723 h out of 8760 h, also indicating that the availability of wave power is 99.58%.

In general, geometry optimisation of WEC systems, based on wave climate, can give an overall evaluation of system performance [73,118,125,127,150]. Some performance criteria, e.g. annual energy production, mean annual power and capacity factor, can only be evaluated based on the wave climate for a given site. As expected, it is time consuming and computation-costly to conduct geometric optimisation based on wave climate. One simplification is to use the most frequent sea state as the design wave condition for evaluating power performance. In order to consider extreme wave loading, system reliability, and survivability, the extreme sea states at the top-right corner of Fig. 3 should be used.

### 3.4. Influence of wave condition on optimal geometry

As wave conditions represent the specific operational environment for WEC devices, their selection has a significant influence on the optimised geometries. For instance, the optimised shape of a hinge-barge AWEC varies significantly for various regular and irregular waves, and wave climates [131]. The optimised shape of a U-shaped OWC based on a wave climate shows significant variation from its counterpart based on a single sea state, and the annual energy production was improved by 4.36% [118] for the more realistic climate case. The selection of design wave conditions should consider both the accuracy and computational cost in evaluating performance criteria. Though harmonic waves are computationally efficient, they can only give an initial approximation of optimal geometry. Irregular waves, based on a specific sea state or wave spectrum (typically the most frequent sea state), is useful to optimise WEC geometry for power absorption. However, the usage of wave climates, based on annual observations, can provide the most representative wave conditions for evaluating mean annual energy production, annual capacity factor, reliability and survivability, of WEC systems. However, the cost in computation is relatively high.

Regardless of specific wave models used, WEC devices are normally optimised for relatively energetic sea states. For some sites of less energetic wave climates, e.g. Mediterranean Sea, some well-known WEC prototypes, e.g. the AquabuOY, Pelamis and Wave Dragon devices, may be somewhat oversized, and more efficient energy conversion can be obtained by optimising the scale factor, which can be achieved through optimisation. A case study is presented in [161], concluding that if the AquabuOY, Pelamis and Wave Dragon devices are scaled down by a factor of 1/2.5, according to the typical wave height and period at Alghero, their capacity factors can be improved from 9% to 20%. In this case study, WEC geometric optimisation by scaling can lead to a smaller hull and a larger capacity factor, indicating a significant reduction in the LCoE.

In addition, long-term trend on wave climate, for example considering a 40 year interval, also has some influence on optimal width and energy absorption of an OWC devices [111], which may assist in cost optimisation. When wave direction is taken into account, the optimal geometry of a submerged planar pressure differential WEC differs from a circular shape [62]. When the performance objectives are related to reliability or survivability [39], extreme sea states should be considered as the design wave condition for geometric optimisation to study extreme wave loads on WEC structure. All in all, the selection of wave conditions has a significant influence on the optimised WEC geometry, but must be carefully chosen, mindful of the performance criteria and computational resources available for optimisation.

### 4. Hydrodynamic modelling approaches

Of the many factors that influence the optimal WEC geometry, the hydrodynamic model plays one of the most crucial roles, and is a major component of any WEC geometry optimisation procedure. Though an accurate PTO model is also required, the level of uncertainty, and variety of possible models, is significantly less than that associated with the hydrodynamic model. PTO modelling issues are discussed in Section 5. In contrast, regarding the hydrodynamic model employed for WEC optimisation, the uncomfortable choice lies between the competing objectives of computational feasibility and modelling accuracy.

A semi-submerged cylinder is taken as an example to illustrate the dynamics of a PA device. As shown in Fig. 4, the motion of the body is governed by Newton's 2nd Law, given as

$$\mathbf{M}\ddot{\boldsymbol{\xi}}(t) = \mathbf{f}_h(t) + \mathbf{f}_g(t) + \mathbf{f}_{pto}(t) + \mathbf{f}_m(t) + \mathbf{f}_{add}(t), \quad (8)$$

where  $\mathbf{M}$  is the inertial matrix and  $\boldsymbol{\xi}$  is the displacement of the WEC.  $\mathbf{f}_h$ ,  $\mathbf{f}_g$ ,  $\mathbf{f}_{pto}$  and  $\mathbf{f}_m$  are the hydrodynamic, gravity, PTO (or control) and mooring forces, respectively.  $\mathbf{f}_{add}$  represents other additional

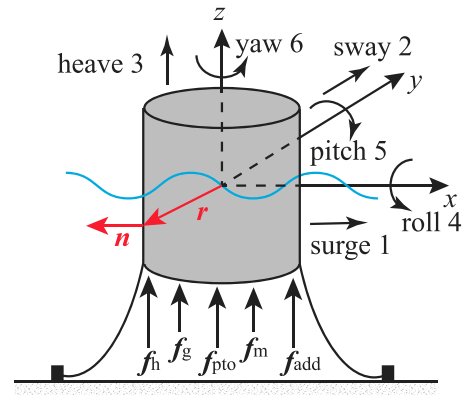


Fig. 4. Hydrodynamics of a semi-submerged cylindrical PA.

forces, e.g. the force induced by end-stop mechanisms. The dimension of these parameters or variables depends on the number of WEC bodies and the number of DoFs considered. As shown in Fig. 4, a WEC body can potentially move in 6 DoFs, including surge, sway, heave, roll, pitch and yaw. For the modes in pitch, roll, and yaw, corresponding components in these force vectors are replaced by torque terms.

For a given wetted surface, the hydrodynamic force or torque can be computed as the integral of the pressure  $p$  on the wetted surface  $S$ , given as

$$\mathbf{f}_{h,i} = \begin{cases} - \iint_S p \mathbf{n} \, dS, & i = 1, 2, 3, \\ - \iint_S p (\mathbf{r} \times \mathbf{n}) \, dS, & i = 4, 5, 6, \end{cases} \quad (9)$$

where  $\mathbf{n}$  and  $\mathbf{r}$  are the normal vector on the wetted surface and the vector of the wetted surface with respect to the reference point, respectively.  $i = 1, 2, 3 \dots 6$  indicates the operation modes in surge, sway, heave, roll, pitch, and yaw, respectively. Here we define  $\mathbf{n}_h = [\mathbf{n}, \mathbf{r} \times \mathbf{n}]'$ .

This section addresses hydrodynamic modelling methods to depict the 'I (interaction)' of WSI, mainly modelling the hydrodynamic force  $\mathbf{f}_h$ , which is one of the critical quantities for wave energy conversion. Hydrodynamic modelling methods, both numerical and experimental, are summarised in Fig. 5. Numerical methods are generally used to solve the Navier–Stokes equations (NSEs) or the Laplace and the Bernoulli equations, as shown in Fig. 5(a), to obtain the pressure  $p$  distribution in the fluid. Hence, the hydrodynamic force or torque can be computed according to Eq. (9). Classification of these hydrodynamic modelling methods are given in Fig. 5(b), where computational fluid dynamics (CFD) is applied to solve the NSEs, with potential flow theory (PFT) used to solve the Laplace and Bernoulli equations. Experimental methods are commonly used to derive empirical models, collect data for system identification, and validate and verify numerical models. Compared to experimental methods, numerical methods are much more cost-effective and amendable for a broad range of WEC applications, including optimisation.

In the literature, there exist several high-quality review papers specifically on WEC modelling only, for example [5–8,162–164]. Detailed modelling methods with case studies are discussed in the book edited by Folley [165]. This section only gives an overview of the aforementioned hydrodynamic modelling approaches for WEC systems, and discusses the pros and cons of each method as they relate to WEC geometry optimisation.

Crucially, while geometric optimisation is only practical for WEC mathematical/computational models (it is clearly impractical to build a large sequence of experimental prototypes), assuring the fidelity of the models employed is important in ensuring that any model-based optimisation is meaningful. To this end, a variety of community-based initiatives have been undertaken, including OES Task 10 [163,166] and CSSP-WSI [167], to address this issue, along with other individual model validation exercises, such as [168,169].

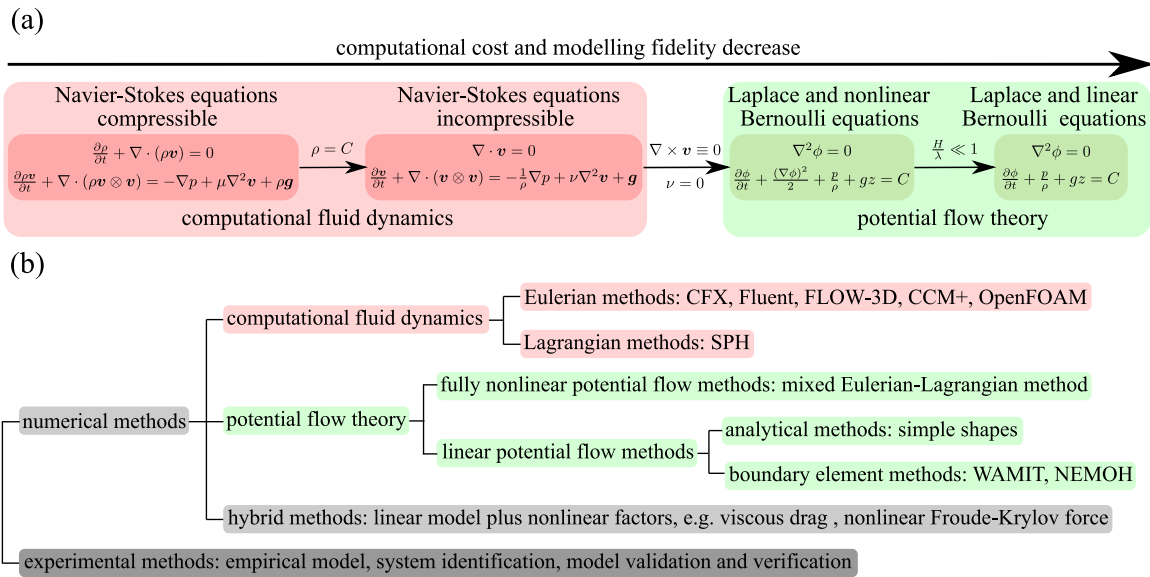


Fig. 5. (a) Governing equations for WEC hydrodynamic modelling and (b) classification of hydrodynamic modelling methods.

#### 4.1. Computational fluid dynamics

CFD packages have been widely applied in WEC applications to provide high-fidelity numerical solutions to WSI by solving the NESs numerically [7]. In Fig. 5(a), the WSI of WEC hydrodynamics is, most generally, governed by the compressible NSEs, given as

$$\frac{\partial \rho}{\partial t} + \nabla \cdot (\rho \mathbf{v}) = 0, \quad (10)$$

$$\frac{\partial \rho \mathbf{v}}{\partial t} + \nabla \cdot (\rho \mathbf{v} \otimes \mathbf{v}) = -\nabla p + \mu \nabla^2 \mathbf{v} + \rho \mathbf{g}, \quad (11)$$

where  $\rho$ ,  $\mathbf{v}$ ,  $p$ ,  $\mu$  and  $\mathbf{g}$  are the water density, particle velocity, pressure, dynamic viscosity, and gravity acceleration, respectively.

The water is generally treated as an incompressible fluid for WEC applications; that is,  $\rho = C$ , where  $C$  denotes a constant. The *incompressible* NSEs can be rewritten as

$$\nabla \cdot \mathbf{v} = 0, \quad (12)$$

$$\frac{\partial \mathbf{v}}{\partial t} + \nabla \cdot (\mathbf{v} \otimes \mathbf{v}) = -\frac{1}{\rho} \nabla p + \nu \nabla^2 \mathbf{v} + \mathbf{g}, \quad (13)$$

where  $\nu = \mu/\rho$  is kinematic viscosity.

Since there are no analytical solutions for the compressible or incompressible NSEs, numerical approaches, comprising the class of CFD methods, are generally applied to obtain numerical solutions or approximations. As computers have become more powerful over the past two decades, CFD methods have been applied more often to solve the NSEs, mainly to compute the pressure and velocity, with the hydrodynamic force or torque then computed according to Eq. (9). Therefore, WEC motion can be determined according to Eq. (8).

CFD methods can be classified into two categories, Eulerian and Lagrangian methods. Eulerian methods, including the finite difference method, the finite element method and the finite volume method, discretise the space and time domains to form a system of linear algebraic equations. On the other hand, the Lagrangian approach discretises the fluid as a set of particles. Both approaches aim to provide numerical approximations of the flow velocity and pressure at the position of each mesh-cell or particle, at each discrete time step. The majority of CFD software packages are based on Eulerian methods, notably ANSYS Fluent, CFX, FLOW-3D, Star-CD/CCM+, and OpenFOAM. In recent years, OpenFOAM has become a widespread tool for WEC applications, mainly due to its flexible and open-source nature. In addition, there exists a large group of researchers and engineers further developing and verifying the OpenFOAM package. Among several Lagrangian

methods, a notable one is the smoothed particle hydrodynamics (SPH) method, with the open-source SPH package, DualSPHysics, available online [170]. However, further experimental verification and validation of DualSPHysics is required. Both categories can deal with compressible or incompressible fluids, depending on the selection of solvers. Note that SPH methods can handle weakly compressible flows accurately, e.g. weakly compressible SPH for OWC modelling [171].

Eulerian-based CFD packages are generally used for modelling WEC dynamics, since they can handle all kinds of nonlinear WEC hydrodynamics, e.g. nonlinear waves, turbulence, overtopping and slamming. A good survey of various CFD methods is given in [7]. Even though the computational cost is high, some examples of CFD methods for hydrodynamic modelling in WEC geometric optimisation exist: CFX was used to optimise the front wall of an OWC [116]; FLUENT was used to optimise the bottom shape of a fix OWC [114] and the ramp shape of a WD device [137]; FLOW-3D was used to optimise the chamber shape of an OWC [117]; OpenFOAM was used to optimise the universal geometry of an OWC device [172] and the profile of the C-cell pitching attenuator [150]; and STAR-CCM+ was used to optimise the underwater shape of an OWC [122].

Lagrangian-based SPH models essentially represent the fluid as a mass of interacting particles, where the interaction between the particles and boundaries is dictated by the governing hydrodynamics. Compared to Eulerian-based CFD methods, SPH methods show advantages in automatic conversation of mass, and simplification of surface tracking. This makes SPH methods particularly suitable for extreme wave events, such as wave breaking. To the best of the authors' knowledge, SPH methods have not, to date, been applied for WEC geometric optimisation, possibly due to computation concerns, though the use of graphical processing units (GPUs) for SPH computation [173] shows promise.

Until now, the only assumption is that water is incompressible, which is generally acceptable for WEC applications. For OWCs, air is included in the power train, which cannot be assumed incompressible. Air compressibility significantly influences OWC performance, e.g. capture width ratio and power output, especially when sea states are energetic and chamber size is large [174–176]. Neglecting air compressibility may under- or over-estimate the power output of OWCs up to  $\pm 30\%$ , depending on wave conditions and PTO damping coefficient [176]. In short, air compressibility should be considered for the hydrodynamic modelling of OWCs of large chamber size (large-scale prototypes) in energetic seas.



CFD software packages have shown good utility for hydrodynamic modelling of WEC systems, with advantages:

- Compared to experimental modelling methods, CFD models are cost-effective to conduct.
- Compared to the potential flow theory, CFD methods consider the fluid viscosity implicitly and intrinsically, and can give high-fidelity modelling results, especially when nonlinear factors dominate WECs' dynamics.
- It is convenient and easy to model various WEC geometries and wave conditions in CFD software packages.

On the other hand, CFD methods are unsuitable for some application scenarios. Some disadvantages are:

- For a learner, CFD software packages are not as direct and friendly as PFT tools, with a steep learning curve.
- The configuration is complex, requiring significant personal experience, with an improper setup potentially leading to large hydrodynamic modelling errors.
- CFD modelling is generally expensive in terms of computational cost, requiring typically 1000 s of computation time for 1 s of simulation time. It may be expected that CFD computational cost will reduce due to the rapid improvement in computing power.

#### 4.2. Potential flow theory

With the assumption of an ideal fluid, i.e. the flow is incompressible, inviscid and irrotational, the NSEs can be simplified to the Laplace and nonlinear Bernoulli equations, as shown in Fig. 5(a). Here, a strong 'simplification' is made, as the NSEs are partial differential equations (PDEs) of the vector  $\mathbf{v}$ , while the Laplace and nonlinear Bernoulli equations are PDEs of the scalar  $\phi$ . A further assumption of small wave steepness  $\frac{H}{\lambda} \ll 1$  is also made. Hence, the quadratic term can be neglected, resulting in the Laplace and linear Bernoulli equations, as shown in Fig. 5(a). Fully nonlinear potential flow (FNPF) theory is associated with the Laplace and nonlinear Bernoulli equations, while linear potential flow (LPF) theory solves the Laplace and linear Bernoulli equations. Both the FNPF and LPF theories are subclasses of potential flow theory (PFT), so named due to the use of the potential function  $\phi$  to obtain the pressure  $p$  in the fluid.

The FNPF theory only assumes the fluid is ideal (incompressible, inviscid and irrotational). Hence, it can handle nonlinear and steep waves, and large body oscillation, but ignores viscosity. Therefore, it is not accurate to say the model derived from the FNPF theory is fully nonlinear. The LPF theory also assumes that the wave height is small with respect to the wavelength, in order to derive the Laplace and linear Bernoulli equations. In addition, it is difficult to solve the Laplace and linear Bernoulli equations if the boundary condition on the wetted surface of the body is nonlinear. Hence, a final assumption is made that the body motion is small, so the normal vectors on the wetted surface of the body can be computed at its equilibrium point, and the WSI is therefore linearised around this equilibrium point.

##### 4.2.1. Fully nonlinear potential flow theory

As shown in Fig. 5(a), the NSEs can be simplified further if  $\mathbf{v} = 0$  and  $\nabla \times \mathbf{v} = 0$  hold, representing inviscid and irrotational flow conditions, producing the Laplace and nonlinear Bernoulli equations, written as

$$\nabla^2 \phi = 0, \quad (14)$$

$$\frac{\partial \phi}{\partial t} + \frac{(\nabla \phi)^2}{2} + \frac{p}{\rho} + gz = C, \quad (15)$$

where  $\nabla \phi = \mathbf{v}$  is the velocity.

The free surface boundary conditions are given as

$$\frac{\partial \phi}{\partial t} + \frac{(\nabla \phi)^2}{2} + \frac{p}{\rho} + g\eta = 0, \quad (16)$$

$$\frac{\partial \phi}{\partial z} = \frac{\partial \eta}{\partial t} + \frac{\partial \phi}{\partial x} \frac{\partial \eta}{\partial x} + \frac{\partial \phi}{\partial y} \frac{\partial \eta}{\partial y}, \quad (17)$$

articulating the dynamic and kinematic free-surface boundary conditions, respectively.

The boundary conditions on the wetted surface of the body and the seabed are given, respectively, as

$$\frac{\partial \phi}{\partial \mathbf{n}} = \mathbf{u}_n, \quad (18)$$

$$\frac{\partial \phi}{\partial z} = 0 \quad \text{at } z = -h, \quad (19)$$

where  $\mathbf{n}$ ,  $\mathbf{u}_n$  and  $h$  are normal vector on the wetted surface of the structure, normal velocity on the wetted surface, and the depth of the seabed, respectively. Here, the assumption of inviscid flow is applied to neglect tangential terms in normal vectors.

The total velocity potential function contains the incident and perturbed parts, that is  $\phi = \phi_i + \phi_p$ . The perturbed part should decay to zero at infinite distance, and, hence, the infinity boundary condition is given as

$$\nabla \phi_p \rightarrow 0, \text{ as } \sqrt{x^2 + y^2} \rightarrow \infty. \quad (20)$$

Due to the presence of quadratic terms in Eqs. (15)–(17), it is difficult to get an analytical solution for the PDEs in Eqs. (14)–(15), subjected to the boundary conditions in Eqs. (16)–(20). In general, numerical solutions or approximations can be obtained via the mixed Eulerian–Lagrangian (MEL) method. The two-stage MEL scheme proceeds at each time step. At the current time step, the potential function and boundary conditions are known, and the first stage is to update the potential function  $\phi$  in the Eulerian frame by solving the Laplace equation through a boundary element method (BEM) or a finite element method (FEM). Thus, the pressure  $p$  can be updated according to the nonlinear Bernoulli equation in Eq. (15). Since  $\phi$  and  $p$  have been updated at the first stage, the secondary stage advances the fluid boundary conditions in the Lagrangian frame according to Eqs. (16)–(17), and (19)–(20). At the same time, the hydrodynamic force or torque can be computed according to Eq. (9), updating the body motion according to Eq. (8) and the wetted surface condition in Eq. (18). That is, the instantaneous wave elevation and wetted surface is used at each time step, requiring re-meshing of the fluid domain at each time step. A relatively fine mesh should be used to reduce modelling error.

Currently, no universal software package is available to solve the Laplace and nonlinear Bernoulli equations, but there are trials for some specific WEC devices. For instance, the HOBEM (high-order boundary element method) package was developed in [115,119], to model OWCs' hydrodynamics using the FNPF theory.

##### 4.2.2. Linear potential flow theory

Assuming the wave steepness is small, i.e.  $H/\lambda \ll 1$ , the nonlinear Bernoulli equation in Eq. (15) can be simplified by neglecting the quadratic term of the potential function. Hence, Eqs. (14) and (15) can be rewritten as

$$\nabla^2 \phi = 0, \quad (21)$$

$$\frac{\partial \phi}{\partial t} + \frac{p}{\rho} + gz = C. \quad (22)$$

Meanwhile, the free surface boundary conditions in Eqs. (16) and (17) can be further linearised by neglecting second-order terms, given as

$$\frac{\partial^2 \phi}{\partial t^2} + g \frac{\partial \phi}{\partial z} = 0, \text{ at } z = 0. \quad (23)$$

For the LPF theory, the wetted surface conditions and the infinite boundary condition are the same as Eqs. (18)–(20). However, small body oscillations are assumed and, hence, the normal vectors in Eq. (18) are computed according to the mean wetted surface, rather than the instantaneous wetted surface used in the FNPF theory.

To solve Eqs. (21)–(22), subject to the boundary conditions of Eqs. (18)–(20) and (23), the total potential function can be divided into incident, diffracted and radiated components, as

$$\phi = \phi_i + \phi_d + \phi_r, \quad (24)$$

where  $\phi_d$  and  $\phi_r$  are the potential functions associated with the diffraction potential assuming the body is fixed at its equilibrium point, and the radiation potential assuming the body is oscillating in still water, respectively. That is, linear superposition is assumed. The pressure can be computed by

$$p = -\rho g z - \rho \frac{\partial \phi}{\partial t}, \quad (25)$$

where  $p_s = -\rho g z$  and  $p_d = -\rho \frac{\partial \phi}{\partial t}$  are the static and dynamic pressure, respectively. Hence, the hydrodynamic force  $f_h$  can be divided into the Froude–Krylov (FK) force  $f_{FK}$ , diffraction force  $f_d$ , radiation force  $f_r$  and hydrostatic force  $f_{hs}$ , given as

$$f_h = f_{FK} + f_d + f_r + f_{hs}, \quad (26)$$

$$f_{FK} = \rho \iint_S \frac{\partial \phi_i}{\partial t} n_h dS, \quad (27)$$

$$f_d = \rho \iint_S \frac{\partial \phi_d}{\partial t} n_h dS, \quad (28)$$

$$f_r = \rho \iint_S \frac{\partial \phi_r}{\partial t} n_h dS, \quad (29)$$

$$f_{hs} = \rho \iint_S g z n_h dS. \quad (30)$$

It is worth noting that (i) the excitation force is defined as  $f_e = f_{FK} + f_d$ , and (ii)  $f_{hs} + f_g = 0$  when a floating WEC body is at rest in still water. When the body deviates from its equilibrium, the hydrostatic pressure provides a restoring force in the modes of heave, roll and pitch, depending on the mismatch between buoyancy and gravity.

For incident linear waves, an analytical solution generally exists. However, analytical solutions for  $\phi_d$  and  $\phi_r$  only exist for some simple WEC shapes, e.g. sphere, cylinder [177,178], etc. For example, a two-dimensional analytical solution is derived and verified in [148], based on a bottom-hinged OWSC device.

For arbitrary WEC geometries, it is difficult to find analytical solutions for  $\phi_d$  and  $\phi_r$ , and BEMs are generally used to obtain numerical approximations of  $\phi_d$  and  $\phi_r$ . The notable BEM solvers are WAMIT, NEMOH, AQWA, AQUA+ and WADAM in the frequency domain, and ACHIL3D in the time domain, with WAMIT, for example, used to compute the frequency-domain response of a spar-buoy type OWC for geometric optimisation [124,125,128]. A comparison study between WAMIT and NEMOH was conducted in [179] by evaluating excitation force, added mass, radiation damping and impulse response function for various WEC concepts. In addition, a good summary of BEMs for wave energy applications is given in [164].

#### 4.3. Hybrid modelling methods

The LPF theory assumes ideal fluid (incompressible, inviscid and irrotational), small wave height and small body motion. These assumptions are acceptable and valid for some offshore structures whose motion is stabilised by design or control. However, it is not the case for wave energy conversion systems as their purpose is to maximise the motion for energy harvesting. Therefore, it is important to consider some key nonlinear factors, depending on WEC concepts, geometric shapes, wave conditions and control strategies. On the other hand, the FNPF theory assumes ideal fluid and, hence, it can handle large (even nonlinear) waves and large body oscillation. However, as the fluid is assumed inviscid, the viscosity effect is excluded. For instance, a truncated cylinder exhibits significant viscous effects both in numerical and experimental testing [180]. In addition, the FNPF theory fails to handle some strong nonlinear phenomena, e.g. viscosity, slamming, overtopping and wave breaking. Ultimately, while CFD methods simulate all

kinds of nonlinear WSI for WEC devices, the computational cost may be too high for some modelling objectives, e.g. annual performance evaluation, typically associated with optimisation activities.

Hybrid modelling methods, in this study, refer to methods that augment the LPF-based Cummins' equation with some nonlinear terms to derive parametrised mathematical models of WEC systems. With the LPF theory, the concepts of excitation, radiation and hydrostatic forces still hold. By superimposing nonlinear terms, better approximation is expected. However, the dominant nonlinear factors depend significantly on WEC geometry and control strategy, and should be carefully considered from case to case. Thus, Cummings' equation [181] can be modified as

$$(\mathbf{M} + \mathbf{M}_\infty) \ddot{\xi}(t) = f_e(t) - \mathbf{K}\xi(t) - k_r(\tau) * \dot{\xi}(t) + f_{pto}(t) + f_m(t) + f_{nl}(t), \quad (31)$$

where  $f_{nl}(t)$  represents nonlinear hydrodynamic forces. Nonlinear treatments can be classified as the following 4 methods:

- **Body-exact treatment:** Instantaneous body motion is considered when computing the FK, diffraction, radiation and restoring forces in Eqs. (27)–(30), while the free surface is linearised at  $z = 0$ , resulting in nonlinear terms in the aforementioned forces. Thus, large body motion is allowed in model modelling.
- **Weak-scatterer treatment:** Instantaneous free surface of incident wave is taken into account while the wetted surface boundary condition is linearised at its mean value, allowing high-order potential functions for computing the forces in Eqs. (27)–(30). Thus, large wave height is allowed for simulation.
- **Viscosity treatment:** The fluid viscous effect is treated by adding a quadratic (Morison [182]) drag term to Cummins' equation. This can significantly improve the modelling accuracy when the relative velocity between the body and fluid is large.
- **Mixed treatment:** This refers to either the body-exact-viscosity treatment, considering both large body motion and fluid viscosity, or the weak-scatterer-viscosity treatment, considering both large wave height and fluid viscosity. For the body-exact-viscosity treatment, there is no universal software package. However, for the weak-scatterer-viscosity treatment, the AQWA package provides an integrated development environment to compute the nonlinear FK and restoring forces according to instantaneous incident wave free surface, together with the drag force according to the Morrison equation [183,184]. The body-exact-viscosity treatment is more generally used for modelling WEC hydrodynamics, as controlled WECs are expected to oscillate in a large stroke range in moderate sea states [51]. Thus, non-linearities induced by large body motion and fluid viscosity are more critical than those induced by large wave height.

Considering both instantaneous wetted surface and free-surface boundary conditions leads to the FNPF theory, and a FNPF model with the viscosity treatment is investigated in [185]. However, the selection of nonlinear treatments is not universal and significantly depends on application scenarios, which will influence their usage for optimisation. A number of nonlinear factors is summarised in [6,186].

Body-exact methods are capable of computing nonlinear FK, diffraction, radiation and hydrostatic forces, and a refined mesh is generally used to avoid re-meshing. However, it may not be necessary to include all nonlinear terms, mainly depending on the geometry of the WEC. For example, when the body size is small, the diffraction and radiation problems can still be solved by the LPF theory, while a body with constant horizontal cross-sectional area will exhibit a largely linear hydrostatic force. A critical aspect is the nonlinear FK force, which has large influence on WEC hydrodynamics [187,188,188,189].

Weak-scatterer methods linearise the free-surface boundary condition at the instantaneous free surface, that is  $z = \eta(t)$ . Therefore, the second-order terms of  $\phi_d$  and  $\phi_r$  (see the nonlinear Bernoulli

equation in Eq. (15) can be added to the diffraction and radiation forces in Eqs. (28) and (29). However, the importance of nonlinear diffraction and radiation terms mainly depends on the body size. For a small body, e.g. a heaving semi-submerged sphere with a radius of 1 m [190], considering nonlinear diffraction and radiation forces shows little improvement in modelling accuracy, but requires significantly more computational resource, which may be prohibitive in iterative optimisation calculations.

The viscosity effect on WEC dynamics is normally included using an empirical term, which is the quadratic drag force in the Morrison equation [182], given as

$$f_v = \frac{1}{2} \rho C_d A (\mathbf{u} - \mathbf{v}) |\mathbf{u} - \mathbf{v}|, \quad (32)$$

where  $A$  is the area normal to the relative flow direction and  $\mathbf{v} = \dot{\xi}$  represents the velocity vector of the WEC body.  $C_d$  is the viscous coefficient. The empirical choice of  $C_d$  is summarised in [191], according to the Keulegan–Carpenter number, the Reynolds number and the roughness number. In addition,  $C_d$  can be determined analytically, numerically or experimentally. However, a wide range of wave conditions should be tested to obtain a consistent value [192]. WEC structures with sharp edges suffer significantly from viscous effects. For instance, both numerical and experimental studies demonstrate that neglecting the viscosity effect significantly exaggerates the RAO of a truncated cylinder [180,193], while undesirable viscous effects can be ameliorated by smoothing the bottom shape [76]. For geometric optimisation, the quadratic drag term is sometimes linearised to an equivalent damping term [29,30,100,194].

Mixed treatment methods can consider fluid viscosity when the body motion or the wave height is large. WEC systems are expected to maximise power output by control in moderate sea, where the body motion is large and the wave height is small to moderate. So, the body-exact-viscosity treatments are useful and handy for modelling WEC dynamics in normal operation mode. For instance, the modelling fidelity of a heaving PA considering nonlinear FK and viscous forces can approach CFD results in OpenFOAM, but the computational cost is significantly lower [195]. Under extreme sea states, WECs are likely to enter a survival mode, e.g. by locking the body. Hence, the weak-scatter-viscosity treatments are seldom used for WEC modelling, and are likely to be relatively inappropriate for geometry optimisation studies.

#### 4.4. Experimental modelling methods

Although numerical methods have many advantages in modelling the WSI of WEC systems, experimental testing is still required and useful for verifying and validating numerical models. In general, small-scale prototypes are preferred at the design stage, as they are cost-effective to manufacture, and easy to test in wave tanks. However, attention should be paid to scaling effects, ensuring the experimental data are capable of reflecting WEC hydrodynamics in real seas. For WEC applications, the Froude number is generally applied which can ensure both the kinematic and dynamic similarities when the Reynolds number is large [196].

For scaled-down prototypes, hydrodynamic forces, body motion, and captured power can be easily scaled up, based on the Froude number. However, mechanical friction is not straightforward to scale up. When a small-scale prototype is used, mechanical friction cannot be scaled down accordingly, and may disproportionately affect experimental results [193]. Hence, a very small scale ratio is not ideal. On the other hand, the scale ratio is also limited by the dimension of wave tanks and cost considerations. If the width, or draught, of a WEC prototype is comparable to the width or water depth of a wave tank, the blockage effect [8] may occur and special efforts are needed to correct experimental data. Thus, scale choice is constrained by the thresholds pertaining to the influence from mechanical friction and the blockage

effect. For example, for the M4 device [129], a comparison study is conducted experimentally addressing the influence of scale ratio on its CWR in regular and irregular waves.

Alternatively, data collected from experimental testing can be used to derive empirical or data-driven models to represent the WSI of WEC devices. Therefore, a wide range of tank testing should be conducted with a wide range of wave conditions to reflect generic hydrodynamic characteristics that WEC systems may experience in real sea. Data-based modelling from physical experiments have been applied to derive mathematical models for various WEC systems [111,113,146,197]. In addition, experimental modelling methods are directly applied for geometric optimisation of some overtopping devices. For instance, the ramp shape of the Wave Dragon devices is optimised by tank testing [134], and the concentrator shape and angle of the SSG device is optimised based on analytical/empirical model from experimental data [141,142].

#### 4.5. Influence of hydrodynamic modelling method on optimal geometry

The choice of hydrodynamic modelling approach for optimisation applications is not straightforward. Some methods can give high-fidelity approximation, e.g. CFD, but also require considerable computation time. On the other hand, simpler models, like Cummins' equation with some nonlinear additions, are not quite mathematically correct. However, Cummins' equation is generally used in offshore engineering, as its approximation accuracy is reasonably good and the computational cost is low for a wide range of offshore applications.

The selection of modelling methods mainly depends on modelling objectives and application scenarios. For instance, large offshore structures are generally stabilised by design and control and, hence, linearisation around an equilibrium point is reasonable. However, WECs with energy maximisation control systems, which work to exaggerate device motion, do not in general satisfy the assumptions for linearisation [51].

CFD methods are useful for comprehensively depicting nonlinear effects of WECs' WSI. However, it is impossible to use them to estimate mean annual power of WECs due to the computational complexity. Nevertheless, annual-based performance criteria, such as mean annual power, annual energy production and capacity factor, are important for WEC design and optimisation. Therefore, a proper hydrodynamic modelling method for geometric optimisation of WECs should, ideally, be both high-fidelity and computationally efficient.

As a hydrodynamic model plays a crucial role, and is a major component of any WEC geometry optimisation, it is to be expected that hydrodynamic modelling methods will have significant influence on the optimised geometry. However, to the authors' best knowledge, the sensitivity of optimised geometries to the nature of the hydrodynamic model used is still an open question. Ultimately, for optimisation applications, a plausible balance between computational complexity and fidelity must be struck, with limited computing power. The degree of nonlinear fidelity required may be a function of the particular WEC topology.

### 5. Modelling of power take-off system

The power take-off is the component in Fig. 1 which transforms the mechanical motion of the WEC into useful energy. Of itself, it does not directly affect the WEC geometry, unless the WEC geometry must be adapted to accommodate the PTO system internally. However, the PTO system has its own dynamics, which allied to those of the floater hydrodynamics, determines the overall frequency response characteristics of the system, which need to be tuned to the relevant sea state(s) via the control system. Therefore, the effect on the overall system dynamics will indirectly influence the optimal device geometry.

Furthermore, the nature of the PTO itself may significantly influence the optimal device geometry, via its effect on the operation of the control system. For example, reactive power flow (where energy is

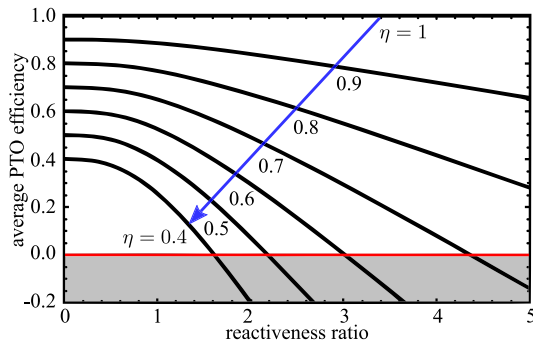


Fig. 6. Average PTO efficiency as a function of the reactance–resistance ratio [202].

taken from the grid to boost device motion) can be used to accelerate the motion of a large device, to tune it into resonance with waves. However, if a PTO only permits unidirectional power flow (from device to grid), then the optimal device is likely to be larger than one where bidirectional power flow is permitted. Further influence of the PTO, via the control system, is considered in Section 7.

In addition to their natural dynamics, and the effect of control forces, the dynamics of the PTO itself may be enhanced by passive mechanisms, i.e. the ‘wavespring’ technology [198] or the snap-through mechanism [199]. These additions can have the desirable effect of reducing reactive power flow and also reducing the PTO peak power rating.

Motion rectifiers, i.e. gearboxes, air turbines, hydro turbines, and hydraulic systems, are generally used to couple the WEC oscillation with generators. Hence, the dynamics of motion rectifiers and generators should be accurately modelled, especially when PTO constraints, such as maximum stroke, force, torque and power, are considered. Significant PTO constraints have been shown to have a marked effect on optimal WEC geometries [33]. Based on some ideal PTO assumptions, the bond graph modelling method [200,201] has demonstrated its feasibility in modelling the dynamics of an hydraulic PTO system and assessing its power output, by assuming the excitation force is known.

However, ideal PTO systems fail to consider some important nonlinear effects in WEC PTO dynamics, e.g. friction, dead-zone, saturation, load effect, hysteresis effect, etc. This may lead to incorrect design decision regarding WEC geometry and the PTO system. For high-fidelity modelling of PTO systems, both the PTO dynamics and efficiency variations with load should be considered. Generators can only operate efficiently under rated (steady) conditions with a peak efficiency lower than 1. In general, the average efficiency of a non-ideal PTO decreases as the reactance/resistance ratio increases [202], as shown in Fig. 6. In addition, the average PTO efficiency decreases dramatically when the load diverges from its rated value. A large amount of energy will also be dissipated by the PTO system, in terms of mechanical loss, copper loss, or hydraulic leakage, which may have an influence on the optimal device shape.

When a mechanical gearbox is used as part of a PTO system, mechanical friction affects the PTO’s dynamics and dissipates some energy. A mechanical motion rectifier (MMR) is tested in [203], to transfer reciprocating WEC motion into uni-directional rotation. The efficiency of the MMR varies from 0.6–0.8, and 40% to 20% energy is dissipated by mechanical friction, respectively. Crucially, the MMR does not easily permit reactive power flow. For hydraulic PTOs, friction losses generally exist in hydraulic cylinders and motors [204]. A case study, based on a hydraulic PTO for a WaveStar-like device, shows that the friction loss is almost as large as the generated electrical power [205]. In addition, experimental data corresponding to a hydraulic PTO system also show some complex nonlinear dynamics, e.g. a hysteresis effect [206]. Air-turbines and hydro-turbines are used for OWCs and overtopping devices, respectively. As the pressure head of

a turbine increases, the mass flow rate increases, but the turbine’s efficiency decreases. Optimised geometry of these devices can increase the pressure head and the mass flow rate. However, this does not mean a higher overall efficiency, if the decrease in turbine efficiency is considered [207].

In practice, PTO losses constitute a crucial aspect that must be taken into account in WEC control, with consequences for the optimal WEC geometry. Different levels of complexity can be used to describe non-ideal PTO behaviour. A complete technical descriptive approach could be employed, leading to a more realistic model, but resulting in a significant increase in computation time, which may be prohibitive in optimisation applications. A simple way is to include PTO losses by means of an efficiency curve or a constant efficiency rate [208]. A high-fidelity wave-to-wire (W2W) model considering nonlinear hydrodynamics, hydraulic dynamics and electrical dynamics are studied in [209]. The systematic complexity is high and a multi-rate solver is required to accelerate the computation. A systematic complexity reduction approach is investigated in [210] to achieve fast computation and modelling.

To date, no comprehensive study of the influence of non-ideal PTO modelling on geometric optimisation of WEC devices is available but, based on the discussion in this section, it should be clear that a co-design framework, considering nonlinear hydrodynamics, non-ideal PTO mechanism and optimal control strategies, is recommended for WEC geometric optimisation.

## 6. Model simplification and implementation

In general, the aforementioned desirable hydrodynamic and PTO modelling characteristics are not straightforward, and simpler parametrised models are preferred for WEC geometric optimisation, given the iterative nature of numerical optimisation. For instance, CFD methods are costly in computation (see Section 4.1), and CFD-in-loop optimisation may lead to unrealistic computing durations. Thus, simplified and parametrised models are required for optimisation, which can be classified into three types, i.e. frequency-domain (FD), time-domain (TD) and spectral-domain (SD) models.

Concerning the hydrodynamic model, in the frequency-domain, Cummins’ equation in Eq. (31) can be rewritten as

$$\{-\omega^2[\mathbf{M} + \mathbf{M}_a] + j\omega\mathbf{B} + \mathbf{K}\}\mathbf{\Xi}(\omega) = \mathbf{F}_e(\omega) + \mathbf{F}_a(\omega), \quad (33)$$

where  $\mathbf{\Xi}(\omega)$  and  $\mathbf{F}_e(\omega)$  are the frequency-domain representations of  $\xi(t)$  and  $f_e(t)$  in Eq. (31), respectively.  $\mathbf{F}_a(\omega)$  represents the control force or/and linear treatments of some nonlinear factors, such as viscous drag, as articulated in Eq. (31). The parameters  $\mathbf{M}_a$ ,  $\mathbf{B}$ ,  $\mathbf{K}$ ,  $\mathbf{F}_e(\omega)$  can be obtained from BEM methods or analytical methods, based on the linear potential flow theory in Section 4.2.2. Such FD models are convenient and computationally efficient, especially when harmonic waves are considered. However, FD models are only valid for ideal PTO systems, where the PTO/control system is represented as some combination of a linear mass–spring–damper system. In addition, it is difficult to consider some nonlinear factors in FD models. However, some nonlinear factors, e.g. viscous force, can be included in FD models with extra effort [211]. In a similar way, SD models can be alternatives to save computing time. Based on the Lorentz linearisation, SD model [212], via statistical linearisation, consider some nonlinear effects, e.g. the viscous quadratic term [29,30,213], nonlinear hydrostatic restoring force and end-stop force [213]. Hence, SD models can statistically and computation-efficiently assess WEC dynamics and power generation for WEC geometric optimisation. However, SD models fail to describe instantaneous WEC dynamics and power capture and, hence, TD models can be preferred when real-time control and physical constraints in WEC/PTO dynamics are indispensable in the optimisation loop.

Compared to FD and SD models, TD models are preferred for some application scenarios, as TD models are capable of handling irregular waves and nonlinear factors in a more flexible manner. In addition,



a wide variety of control systems can be simulated, which may give more meaningful overall description of the WEC performance for different geometric configurations. In the time domain, the dynamics of a WEC system is often represented by Cummins' equation in Eq. (31), which contains a convolution radiation force term, which is not efficient in computation. A first attempt, therefore, to simplify the model computationally, is to approximate the convolution term by a finite-order parametrised model, e.g. a state-space model. Such a radiation approximation can be implemented by a variety of system identification techniques [214–219].

Starting with a nonlinear TD model, there are various approaches to reduce the model to a form which is amenable to numerical optimisation, while still retaining key nonlinear characteristics. Specifically, methods in [210,220] describe procedures which may be used to reduce the complexity of nonlinear hydrodynamic and PTO models in a progressive way to allow a specific complexity/fidelity trade-off to be achieved, while retaining specific nonlinear characteristics.

Another way to produce a parametrically compact (linear or nonlinear) model for optimisation is to use data collected from a computationally complex high-fidelity model [209] to be used in a subsequent system identification procedure [221]. The discrete-time data can be used to produce both continuous-time [222] or discrete-time [221] (black-box) parametric models, at a complexity level scalable by the user, both in terms of degree of nonlinearity and dynamical order, which is ideal for geometric optimisation, where computation is limited.

System identification techniques can be applied where aspects of the model are well known, or where the model structure is known, but the parameter values are uncertain [223]. This leads to the so-called grey-box modelling, where the various shades of grey denote the level of *a priori* knowledge available [224], with white-box denoting a complete first-principles model and black-box denoting the complete absence of physical information.

While LPT produces linear WEC models which are linearised about the device equilibrium point, and assume small variations about that equilibrium (a challenging assumption in an application where the objective is to exaggerate motion), in WEC applications, system identification can be used to identify linear models which are more representative over the full operational space [225]. Other examples of system identification applied in the wave energy application, utilise both linear and nonlinear model structures, e.g. [226]. When identifying parametric models from system identification experiments, care needs to be taken to cover the complete operational space of the device, in both motion (displacement, velocity) and frequency [227].

Based on input–output relation, WEC dynamical models can be classified as force-to-motion (F2M), wave-to-motion (W2M) and W2W models, as follows:

- F2M models focus on the WSI radiation problem of WECs (also including inertial and restoring effects) and can, for example, be derived analytically based on Cummins' equation in Eq. (31) [193, 218,219], or identified from numerical or experimental data by externally forcing the body oscillate in still water [226,227], noting that decay testing only depicts the radiation problem around the natural frequency of a WEC device. Numerical simulation of F2M models assumes that the excitation force is known, and the output signal is usually either displacement or velocity.
- W2M models include the F2M dynamics, but also includes the excitation process dealing with the incident and diffraction problems, noting that the physical process from wave elevation to wave excitation force is typically non-causal. In practical WEC implementation, the excitation force *cannot be measured directly*, since it cannot be decoupled from other hydrodynamic forces for an oscillating body [228]. It is also noteworthy that knowledge of the excitation force is critical in the generation of optimal velocity reference signals for WEC control systems, and can be estimated or approximated [228–235]. Alternatively, W2M models can also be directly identified from CFD or experimental data [197,226, 227], by which the non-causal process is implicitly handled.

- W2W models include both WSI and structure–PTO interaction, and can depict all the three power transfer stages given in Fig. 1, having the advantage of displaying useful power output, which may be key in realistic geometry optimisation. Thus, W2W models provide the possibility to include more realistic non-ideal PTO models. While a number of W2W modelling approaches are summarised in [6,11,236], only a few W2W models consider the nonlinear coupling between hydrodynamics and control [237, 238]. A systematic complexity reduction approach is investigated in [210] and concludes that W2W models can be simplified according to modelling purposes. For the purpose of power assessment (a typical metric in WEC geometry optimisation), it is suggested that the dynamics of a non-ideal hydraulic PTO system can be neglected and an efficiency curve can be used to represent PTO losses for system complexity reduction [208,210].

In summary, for WEC geometric optimisation, the straightforward application of complex hydrodynamic and PTO models in the optimisation loop may lead to unacceptable computing time. Hence, model simplification is useful to parametrise WEC models, as FD, TD and SD models, for optimisation implementation. FD and TD models are widely applied, and only a few studies use SD models. W2M models are generally used, by assuming ideal mass–spring–damper systems for PTO dynamics. A more realistic W2W model for geometric optimisation should simultaneously consider critical nonlinear hydrodynamics, non-ideal PTO dynamics and real-time control with physical constraints. Such a model is expected to have a high systematic complexity, but further model simplification can be achieved according to application scenarios [210].

## 7. Control strategies

As ocean waves are irregular with varying amplitude and frequency, and sea states change from time to time, control approaches are required by WEC systems for power maximisation in moderate sea states and survivability enhancement under extreme wave conditions. In general, a properly designed control strategy tends to exaggerate the oscillation of a WEC device, which, in turn, can invalidate the assumptions of the LPF theory [51,239]. Hence, nonlinear forces, e.g. viscous and FK forces are typically exaggerated by control, and WEC geometric optimisation should include the effect of control. A wide range of WEC control strategies are available, e.g. reactive control and phase control [240], optimisation-based control [10], adaptive control [241, 242], etc. This section only discusses some basic concepts of WEC control, focusing on their influence on WEC geometric optimisation. For detailed review on control, readers are referred to [9–12].

### 7.1. Classic control strategy

To derive classic control methods, Cummins' equation in Eq. (33) can be rewritten as

$$\frac{V(\omega)}{F_e(\omega) + F_{pto}(\omega)} = \frac{1}{Z_i(\omega)}, \quad (34)$$

where  $V(\omega)$  represents the body velocity in the frequency domain.  $Z_i(\omega)$  is the intrinsic impedance of the system,

$$Z_i(\omega) = B(\omega) + j\omega \left[ M + M_a(\omega) - \frac{K}{\omega^2} \right]. \quad (35)$$

According to the maximum power transfer theorem, the optimal PTO system should satisfy

$$Z_{pto}(\omega) = Z_i^*(\omega). \quad (36)$$

That is, the maximum absorbed power by the PTO system is achieved when the PTO impedance is the complex conjugate of the system intrinsic impedance. Such a control method is called the complex conjugate control or reactive control (RC) [240]. For reactive PTO/control

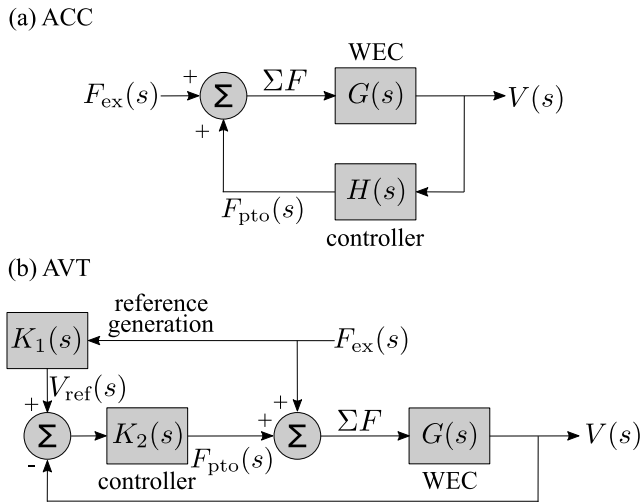


Fig. 7. Control structures for (a) approximate complex conjugate (ACC) and (b) approximate velocity tracking (AVT) [12].

systems, bi-directional power flow is required. However, some PTO systems only allow uni-directional power flow, represented therefore as pure dampers, resulting in the so-called passive control (PC), given as

$$B_{pto}(\omega) = |Z_1(\omega)|. \quad (37)$$

Based on the reactive control law in Eq. (36), the optimal velocity is given as

$$V_{opt}(\omega) = \frac{F_e(\omega)}{2B(\omega)}, \quad (38)$$

which indicates that the absorbed power is maximised if the WEC velocity is proportional to the excitation force. Control laws based on this equation include phase control [240], which can be achieved by latching control (LC) or declutching control (DC).

For WEC geometric optimisation, classic control methods are generally used, usually giving a simple parametric form for the controller. For instance, reactive control is applied in [78,130]; passive control is used for geometric optimisation of pitching PAs in [96,104] and OWCs in [114]; and phase control by latching and declutching are applied in [53,194]. The ideal latching/declutching time, and corresponding optimal damping value during the free response, have been studied by a variety of researchers, including [243–245]. For passive control, the PTO damping coefficient is typically selected at the peak frequency of a given spectrum [246].

### 7.2. Modern control strategies

Classic control methods calculate the optimal conditions for power maximisation of linear WEC devices in monochromatic waves. However, more realistic WECs contain nonlinear hydrodynamics, non-ideal PTO systems and are subject to irregular waves. In general, reactive and phase control concepts can be extended to panchromatic waves under the frameworks of approximate complex conjugate (ACC) and approximate velocity tracking (AVT) [12], shown in Fig. 7.

The AVT framework is more flexible than the ACC one, permitting the incorporation of physical constraints, and is generally used for the majority of optimal control strategies, but requires knowledge of the excitation force. Without loss of generality, the WEC control problem can be reformulated as an optimal control problem, given as

$$\begin{aligned} \min_{f_{pto}} & - \int_0^T f_{pto}(t) v(t) dt \\ \text{subject to} & \xi(t) \leq \xi_{max}, \\ & f_{pto}(t) \leq f_{max}. \end{aligned} \quad (39)$$

Based on this formulation, several optimal control algorithms are summarised in [10]. However, only a few studies consider modern control methods in WEC geometric optimisation, possibly due to the increased computation time associated with numerically optimal control. For example, pseudo spectral optimal control (PSOC) is applied to optimise the shape of heave PAs in [33,60], and the influence of control methods, including DC, LC, PC, and PSOC, on geometric optimisation is assessed in [33,64].

In addition, modern control methods can handle the constraints in a more flexible manner [33]. However, there are very few studies discussing the existence of optimal solution under physical constraints. Based on the PSOC algorithm, a geometric tool is developed in [247], to discuss the existence of optimal solution subject to constraints in PTO displacement and force. As shown in Fig. 8(a), the optimal power output can be achieved when the maximum values of the position and force constraints are large, or when the excitation force is relatively small. However, the suboptimal power may differ from the optimal constrained solution if the maximum values of the constraints decrease or the excitation force increases, as shown in Fig. 8(b). If the maximum values of the constraints decrease further or the excitation force increases further, neither optimal nor suboptimal solutions exist, as shown in Fig. 8(c).

In Fig. 8, the constraints mainly depend on the design or selection of PTO systems, and the excitation force depends on wave conditions and WEC geometry. Hence, the existence of an optimal solution will be affected by the PTO system specification, wave climates, WEC geometries and hydrodynamic modelling methods. This interaction strongly suggests a co-design framework for WEC geometric optimisation.

### 7.3. Influence of control strategy on optimal geometry

Control units act as a ‘bridge’ connecting WEC hydrodynamics with PTO dynamics. In turn, control strategies have a significant influence on the dynamics of the WEC body and PTO components, and consequently affect the optimised WEC geometries. In general, WEC controllers are based on linear WEC models with several assumptions, i.e. ideal fluid flow, small body motion and small wave height (see Fig. 5). However, power maximisation control strategies tend to enlarge the body motion, which invalidate these assumptions. Hence, nonlinear effects should be treated in a proper way [51], to achieve high-fidelity modelling without high computational cost. As shown in Fig. 9(a), latching control exaggerates the motion orbit dramatically, and a hybrid modelling method with treatment of nonlinear FK and viscous drag forces (marked NLFKaD) gives results approaching the fidelity of CFD via OpenFOAM, while other methods fail to model WEC motion accurately. In addition, the computation time of the NLFKaD method is considerably less than that for CFD methods, as shown in Fig. 9(b), and the NLFKaD method is recommended for WEC geometry optimisation when power maximisation control is applied. In Fig. 9(b),  $t_{cpu}$  is the computation time.

As expected, power maximisation control strategies significantly affect WEC hydrodynamic optimisation, and the optimal geometry is therefore sensitive to the control method employed. For example, an optimised truncated cylinder harvesting wave energy in heave has much larger dimensions and natural period for passive control than for latching control [53]. A broader comparison study of the control influence on geometric optimisation is discussed in [64], in which the optimised shapes of uncontrolled, latching-, declutching- and PSOC-controlled devices differ from each other dramatically. In addition, the PSOC strategy, a representative of modern control strategies, outperforms the other control methods [64], and the optimised geometry using the PSOC strategy shows higher robustness to varying sea states than the other control approaches.

In addition, physical PTO constraints, which are not considered by all control methods, have some influence on the optimised geometry. A larger value in stroke or power constraint will lead to a larger displaced volume for devices [151,152]. Similar conclusions are drawn in [33], where a tight constraint in PTO force leads to a smaller dimension of an optimised cylinder operating in heave.

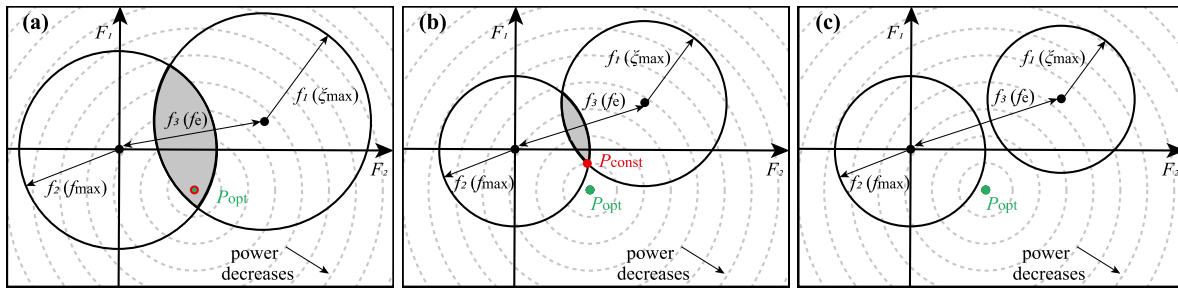


Fig. 8. Effect of constraints on optimal control: (a) no effect on optimal power output when the optimal solution is situated in the overlapping region; (b) optimal power output with constraints is lower than that without constraints when the optimal solution is situated outside of the overlapping region; and (c) there exists no optimal solution to satisfy constraints if there is no overlapping region. This figure is inspired by the development in [247].

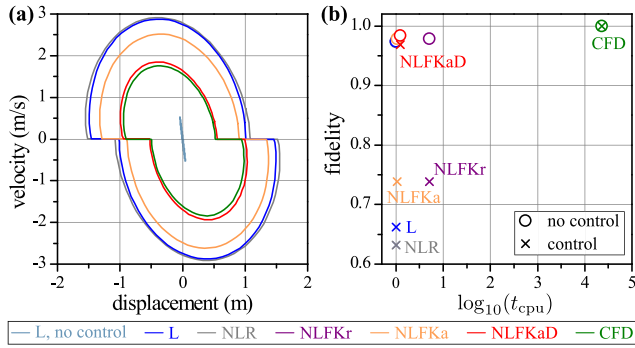


Fig. 9. Comparison of phase portraits (a), and modelling fidelity against computation cost (b), for a heaving sphere in regular waves of height 1 m and period 6 s for a variety of modelling approaches with/without latching control [51].

### 8. Optimisation criteria

To assess the performance of a WEC concept, a variety of metrics have been used to evaluate its TPL and TRL. For successful commercialisation, the concept should be of technological and economical viability [248]. Correspondingly, criteria for WEC geometric optimisation should consider both the technological and economic performance. The performance criteria for WEC geometric optimisation can be classified into the following three types: (i) economic criteria, (ii) technical criteria, and (iii) techno-economic criteria. This section will introduce these criteria, discuss their influence on WEC geometric optimisation, and assess their practicality as optimisation targets. However, given the sensitivity of the optimal geometry to the performance goal, the choice of performance function is key in achieving realistic optimal shapes, while also requiring to be computationally tractable.

#### 8.1. Economic criteria

While the energy in waves is ostensibly free, the technology used to harness it is not and the cost of delivered wave energy is the ultimate arbiter of its adoption. Key economic criteria include the levelised cost of energy (LCoE), the net present value (NPV), the internal rate of return (IRR), and the discounted pay back period (DPBP). In this study, these economic criteria follow the definition in [249], and only an overview is given in the following.

The LCoE over the life-cycle of a WEC project can be defined by the present value (PV) approach, given as

$$LCoE = \frac{PV(CapEx) + PV(OpEx)}{PV(AEP)}, \quad (40)$$

where *CapEx*, *OpEx* and *AEP* are capital expenditure, operation and maintenance expenditure, and annual energy production, respectively.

The present value of cash flow (CF) is defined as

$$PV(CF) = \sum_{y=y_0}^Y \frac{CF(y)}{\left(1 + \frac{R_d}{100}\right)^y}, \quad (41)$$

where  $R_d$  and  $y$  are the discount rate and the year index, respectively, with the life-cycle running from  $y_0$  to  $Y$ . Estimates of the CapEx, OpEx and LCoE for early commercial scale WEC project are 2700–9100 \$/kW, 70–300 \$/kW per year, and 120–470 \$/MWh in [250], respectively, with detailed calculation and estimation methods given in [249–251]. However, large uncertainties exist in these estimates, given that limited operational experience of WEC projects is available. These estimates are based on average values for various WEC devices and cannot reflect the LCoE for a specific WEC project. In addition, the capacity factor is optimistically assumed to be around 0.3 [250], while an operating OWC wave farm can only achieve a capacity factor of about 0.11 [22]. On the other hand, long-term projections, considering learning rate, conclude that the LCoE tends to decrease to 100–150 \$/MWh as the cumulative installation capacity increases to 10 GW [250]. This reveals the rationality for policy makers to applying renewable energy feed-in tariffs (REFITs) to encourage private investment.

The free cash flow (FCF) can be defined as

$$FCF(y) = \frac{Rev(y) - CapEx(y) - OpEx(y) - Tax(y)}{\left(1 + \frac{R_d}{100}\right)^y}, \quad (42)$$

where *Rev* is the annual revenue, containing the REFIT, if available, and *Tax* representing annual taxes. Therefore, the NPV, IRR and DPBP can be calculated by

$$NPV = \sum_{y=0}^Y \frac{FCF(y)}{\left(1 + \frac{R_d}{100}\right)^y}, \quad (43)$$

$$\sum_{y=0}^Y \frac{FCF(y)}{\left(1 + \frac{IRR}{100}\right)^y} = 0, \quad (44)$$

$$\sum_{y=0}^Y \frac{FCF(y)}{\left(1 + \frac{R_d}{100}\right)^y} \geq 0. \quad (45)$$

Private stockholders may use the NPV, IRR and DPBP to make decisions on their investment on WEC projects. Sensitivity analysis shows that the REFIT has a significant influence on the NPV and IRR, and a relatively higher REFIT can lead to profitable wave farm projects [249,252]. In addition, NPV is applied as an optimisation criterion for a barge-type attenuator in [130], and the optimised number is much smaller than its counterpart by using a purely technical criterion.

Though the criteria in Eqs. (40)–(45) have quite complex relationships with the device geometry, some studies on WEC hydrodynamic optimisation adopt these criteria as the cost function in the optimisation loop. For instance, the LCoE is used to optimise the radius of a heaving point absorber in [102] and the hull structure of a BBDB

device in [127]. The per-kWh cost of the all-electrical chain (excluding geometry) for the SEAREV device can be minimised by particle swarm methods [253]. On the other hand, WEC optimisation based on these economic criteria remains a challenging task [248]. Given that operational experience in this sector is severely limited, a high level of uncertainty exists in the estimation of the criteria in Eqs. (40)–(45). For instance, the calculated LCoE for the Pelamis device varies from 0.05–0.30 €/kWh, depending on wave climate, material prices, installation cost, rated power, REFIT, etc [252].

### 8.2. Technical criteria

Technical criteria for evaluating the performance of WEC systems can directly reflect the TPL of WEC concepts, which include the power-related, energy-related, efficiency-related and natural-frequency-related criteria, and generally have a more direct relationship with the device geometry than purely economic criteria. Without loss of generality, the average absorbed power,  $P_a$ , can be written as

$$P_a = \frac{1}{T} \int_0^T f_{pto}(t) v(t) dt, \quad (46)$$

where  $T$  is the time span, which can be several seconds for regular waves, hundreds of seconds for irregular waves, and months/years for wave climates. Maximising average power absorption is often used for many kinds of WEC devices, for example [28,62,118,125,128]. Some studies even seek to achieve multiple objectives, e.g. shape optimisation of the SEAREV device aims to maximise the absorbed power and to minimise the displacement simultaneously [96].

Another generally used technical criterion is energy production,  $EP$ , given as

$$EP = \int_0^T f_{pto}(t) v(t) dt. \quad (47)$$

When the time span  $T$  is annual, this equation results in the annual energy production (AEP), which is broadly used to evaluate the performance of a WEC device at a specific site, or to compute the LCoE defined in Eq. (40). In addition, the AEP can also be used as the objective for shape optimisation [102,104].

Historically, the hydrodynamic efficiency of a WEC device is mainly represented by the capture width ratio,  $CWR$ , given as

$$CWR = \frac{P_a}{JL_c}, \quad (48)$$

where  $J = J_r$  or  $J = J_{ir}$  for regular or irregular waves, respectively.  $L_c$  is the characteristic dimension of a WEC device, normally the width of the device with respect to the wave front. To make the CWR more comparable among a variety of WEC devices, the characteristic dimension can be modified by the cube root of displaced volume [145], or the square root of the submerged surface area [93,95]. The CWR is frequently accepted as a measure of hydrodynamic efficiency [112,113], and also alternatively denoted as the capture factor [145], or relative capture width [241]. For WEC geometric optimisation, the CWR is widely used as the maximisation objective for all types of WEC systems, see [109,111,113,115–117,119,123,145,148,149,172]. Based on similar concepts, a performance criterion, denoted the *overtopping rate*, is specified to represent the hydrodynamic efficiency for optimising overtopping WECs, e.g. the Wave Dragon device [134,136,144].

More simply, some studies try to match the natural frequency of a WEC system to the incident wave [70,82], by evaluating the RAO as the performance index.

$$RAO = \frac{A}{H/2}, \quad (49)$$

where  $A$  is the amplitude of WEC displacement. However, such an exercise does not consider the beneficial effect of control in broadening the WEC bandwidth, as documented in Section 7.

### 8.3. Techno-economic criteria

The economic criteria in Eqs. (40)–(45) are based on estimated values of CapEx, OpEx and AEP from some preliminary WEC projects, and it is assumed that technical measures on improving the AEP have no influence on the CapEx and OpEx. However, this is not true. For instance, power maximisation control can improve the AEP significantly, but it may also increase the peak-to-average power ratio, resulting in a high rated power but a low capacity factor for PTO units, leading to a higher LCoE and a lower NPV [254]. In addition, the technical criteria in Eqs. (46)–(49) only focus on improving the absorbed power or hydrodynamic efficiency, but neglect the influence of optimisation design or control on the cost. Power-oriented shape optimisation may result in a large structure and, hence, an unacceptably large value of CapEx. Power maximisation control, e.g. reactive control, may lead to a large peak-to-average power ratio, which can significantly increase PTO cost. Therefore, it is critical to consider both economic and technological criteria for WEC geometric optimisation.

A novel framework to assess both the productivity and economic feasibility of WEC projects is proposed in [249]. As shown in Fig. 10, this method combines a cluster of models to reflect the WEC operational environment, manufacture, deployment, operation and maintenance, and productivity. The resulted CapEx, OpEx and AEP are fed into a financial calculator to compute the economic criteria. However, it is difficult to adopt this framework for WEC geometry optimisation, as these techno-economic criteria consider a wide range of parameters for optimisation, including: (i) design parameters, e.g. geometric structure, (ii) control parameters, e.g. PTO constraints, (iii) operational parameters, e.g. wave climate, (iv) economic parameters, e.g. the cost of material and the REFIT, and (v) market data, e.g. price of electricity. Such a multi-objective and multi-parameter optimisation problem may be computationally intractable.

Some simplifications can be made to represent techno-economic criteria by assuming the CapEx and OpEx are proportional to characteristic parameters of WEC's geometry, e.g. submerged surface area, displaced volume, and characteristic length. Average absorbed power per submerged surface area ( $P_s$ ), average absorbed power per displaced volume ( $P_v$ ), and average absorbed power per displaced mass ( $P_m$ ), can be defined as

$$P_s = \frac{P_a}{A_s}, \quad (50)$$

$$P_v = \frac{P_a}{V_d}, \quad (51)$$

$$P_m = \frac{P_a}{M}, \quad (52)$$

where  $A_s$ ,  $V_d$  and  $M$  are the submerged surface area, the displaced volume and mass, respectively. Alternatively, annual energy production per submerged surface area, displaced volume and mass, can be written as

$$AEP_s = \frac{AEP}{A_s}, \quad (53)$$

$$AEP_v = \frac{AEP}{V_d}, \quad (54)$$

$$AEP_m = \frac{AEP}{M}. \quad (55)$$

If annual data are used to compute the power-related criteria in Eqs. (50)–(52), these criteria will show the same trends as the AEP-related criteria in Eqs. (53)–(55). In addition,  $P_v$  and  $AEP_v$  are the surrogates of  $P_m$  and  $AEP_m$ , respectively, since  $M = \rho V_d$ . Some preliminary WEC geometric optimisation studies use these aforementioned techno-economic criteria as optimisation objectives, for example [93, 107,147,194]. However, these studies do not reveal the rationale of using these criteria as simplified representatives of LCoE.

Intuitively, these techno-economic criteria in Eqs. (50)–(55) reflect the efficiency of utilising the WEC structure. A preliminary study, based



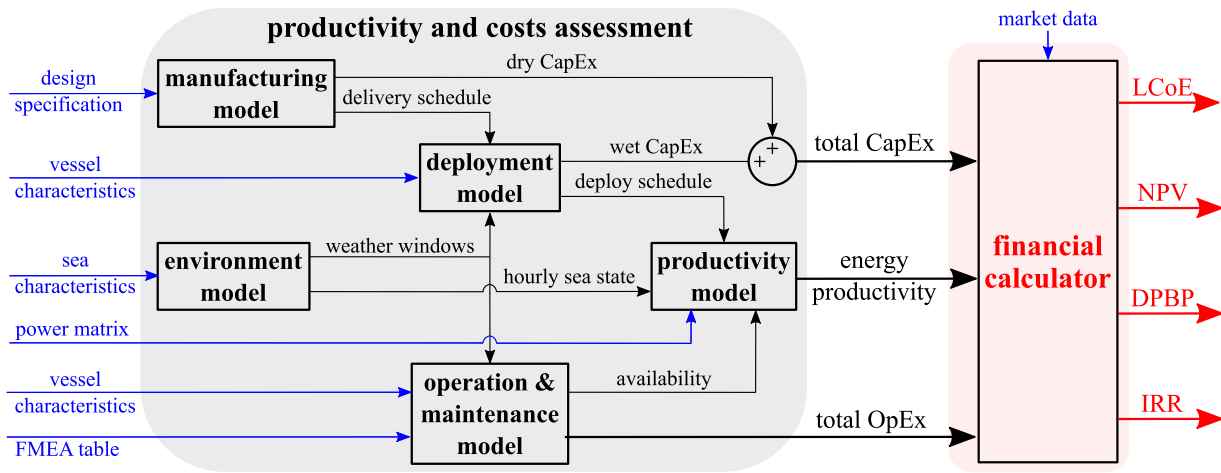


Fig. 10. Schematic of a wave farm productivity and financial calculator [249].

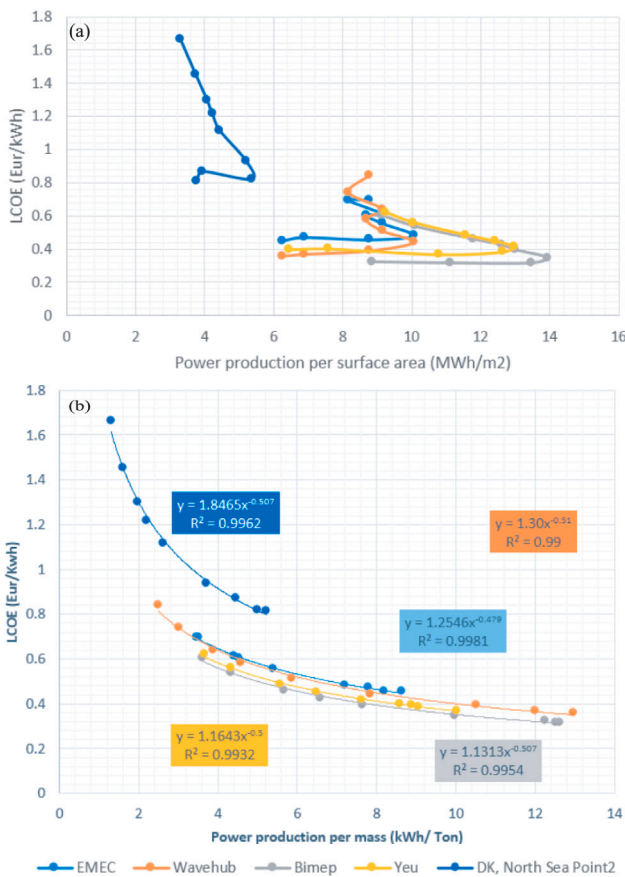


Fig. 11. Variants of LCoE with changes in (a) the energy production per  $m^2$  of submerged surface area, and (b) the energy production per unit mass [254].

on a wave farm of CorPower devices with an installation capacity of 20 MW [254], shows clearly that LCoE is strongly related to the simplified techno-economic criteria. As shown in Fig. 11(a), a maximum value of  $P_s$  generally achieves a low LCoE around its minimum value, regardless changes in wave climate. Fig. 11(b) further illustrates that the LCoE decreases monotonically as  $AEP_m$  increases, i.e. a maximised  $AEP_m$  always results in a minimised LCoE. This is the rationale of using these simplified techno-economic criteria for WEC geometric optimisation.

Compared to the complex techno-economic schematic in Fig. 10, the simplified techno-economic criteria in Eqs. (50)–(55) are computationally feasible for WEC geometric optimisation, and the optimised geometry is expected to be more realistic than that based on purely technical criteria in Eqs. (46)–(49). When the PTO reliability is considered, optimisation criteria should include the PTO force or torque. For instance, average power per PTO force is used in [39,194,255] and the ratio between the maximum reaction force and the maximum absorbed power is adopted in [147]. In [79], the LCoE is simplified to  $AEP_m^{-0.5}$ . Thus, minimising the LCoE in [79] is equivalent to maximising the  $AEP_m$  in Eq. (55).

#### 8.4. Influence of optimisation criterion on optimal geometry

Naturally, it is difficult to determine a universal optimisation criterion for geometric optimisation of all kinds of WEC systems. For successful commercial applications, economic criteria are paramount for policy makers and stockholders. However, these indices are of high uncertainty, mainly limited by little operational experience of WEC projects. On the other hand, technical criteria are broadly used for improving WEC performance by geometric optimisation or/and control, but are insensitive to CapEx and OpEx. In reality, technical criteria have a significant influence on economic criteria. For instance, reactive control can dramatically improve AEP, but may not lower LCoE, since reactive control induces a high level of reactive power and a large peak-to-average power ratio in power flow. As a consequence, the rated power increases, the capacity factor decreases, and the possibility of component failure increases. Thus, both the CapEx and OpEx increase and the LCoE may be increased, rather than decreased.

Techno-economic criteria inherently compromise both economic and technical objectives, and typically transform the problem of LCoE minimisation to the problem of maximising the absorbed power or energy per characteristic dimension. The study in [254] has demonstrated the feasibility and validity of such a simplification, at least for the CorPower device. However, these simplified criteria may lead to a relatively small geometry, and extra metrics, such as delivered power, should be included to form a multi-objective optimisation problem. When the reliability of a PTO system or components are considered in relation to OpEx, penalty functions of large PTO force or torque should be taken into account in the optimisation cost function. When multiple objectives compete with each other, and are unrealistic to combine in a single performance function, a Pareto front can be used to find the optimal multi-objective solution [96,253,256]. The main advantage of the Pareto optimisation is that the sensitivity of the relationship between competing metrics is revealed, providing the designer with useful information to make a final decision. However, given that

expert user intervention is usually required to interpret the Pareto result, this approach does not lend itself easily to automated numerical optimisation.

As expected, the choice of optimisation criterion has a significant influence on the ‘optimal’ WEC geometry, as documented for example in [92–95,106,130,147]. An interesting finding in [152] is that optimisation criteria of average power, average power per characteristic length and average power per volume result in large-, medium- and small-sized hulls, around 3000 m<sup>3</sup>, 1000 m<sup>3</sup> and 300 m<sup>3</sup>, respectively. By comparing the economic-criterion-driven, the technical-criterion-driven and the weighted-driven optimisations [257], the first approach always leads to a small hull, and the second method results in a large hull, while the weighted one considering both types of criteria converges to a median buoy size.

## 9. Optimisation algorithms

Without loss generality, the geometric optimisation problem of WEC systems can be formulated as

$$\begin{aligned} & \min_{\mathbf{X}} F(\mathbf{X}) \\ \text{subject to } & \mathbf{H}(\mathbf{X}, \boldsymbol{\xi}, \boldsymbol{\eta}) = \mathbf{0}, \\ & \mathbf{C}(\mathbf{X}, \boldsymbol{\xi}) \leq \mathbf{0}, \\ & \mathbf{X}_l \leq \mathbf{X} \leq \mathbf{X}_u, \end{aligned} \quad (56)$$

where  $F(\mathbf{X})$  is the cost/performance function which, in general, cannot be expressed in an explicit algebraic form, but can be numerically computed.  $\mathbf{X}$  represents the design parameters in the design space of  $[\mathbf{X}_l, \mathbf{X}_u]$ , while  $\mathbf{H}(\mathbf{X}, \boldsymbol{\xi}, \boldsymbol{\eta}) = \mathbf{0}$  and  $\mathbf{C}(\mathbf{X}, \boldsymbol{\xi}) \leq \mathbf{0}$  represent the hydrodynamic and control constraints, respectively. Before the optimisation process, the following needs to be considered: (i) modelling fidelity and computational resource availability; (ii) properties of the optimisation problem, such as continuous or discrete, single or multiple objectives, deterministic or stochastic, constrained or unconstrained; (iii) properties of the design space, e.g. number of local optima, discontinuity; and (iv) constraint handling.

A plethora of optimisation algorithms is available, with no unique classification method to cover the broad range of possibilities. The appropriate choice of optimisation algorithm is somewhat problem dependent, and there is no universal methodology to choose the ‘best’ algorithm for all problems. Equally, there is no single optimisation algorithm which is suitable for all problems. A variety of optimisation algorithms for aerodynamic optimisation is summarised in [258], within which the algorithms are classified into three categories: gradient-based, gradient-free and hybrid algorithms. Shape optimisation of WEC systems share some similarity with aerodynamic optimisation and some experience from aerodynamic optimisation may be relevant for WEC hydrodynamic optimisation. On the other hand, shape optimisation of WEC systems appears more complex, as a realistic procedure should consider the interaction among stochastic wave climates, nonlinear hydrodynamics, optimum control strategies, non-ideal PTO dynamics and uncertain market data, to minimise the LCoE. In addition, WEC geometry optimisation involves 2-phase flow, compared to the single phase case in aerodynamics.

WEC shape optimisation aims to obtain the most suitable shape under a given set of conditions, including WEC structure, wave conditions, hydrodynamic model, PTO dynamics, power maximisation control approaches, and performance criterion employed. In general, this optimisation problem is multi-parameter and multi-objective, and subject to a variety of constraints. Some specific cases may present a convex optimisation problem. However, in general, solution spaces may have multiple optima and special care should be taken to determine an acceptable solution. However, many global search methods, such as evolutionary or genetic algorithms (EAs and GAs, respectively) consume considerable computational resources.

As the cost function  $F(\mathbf{X})$  in Eq. (56) is implicit, multi-parameter, multi-objective and iterative, it may be challenging to find the global optimal solution. In general, optimisation algorithms can be divided into the exhaustive search methods (ESMs), local search methods (LSMs) and global search methods (GSMs). This paper only considers the application and influence of optimisation algorithms on optimised geometry. For a detailed mathematical description of optimisation algorithms, readers are referred to [259,260].

### 9.1. Exhaustive search

An exhaustive search method is the simplest algorithm to find the optimum solution when the design parameters are discretised on a space. When the number of design parameters is small and the design space is limited, it can be an effective approach, and also provides information in the neighbourhood of the optimum, indicating sensitivity of the performance function to the optimised parameters, and is almost guaranteed to find the global optimum. For multi-parameter cases, subsequent single-parameter studies can be iteratively used to find the global optimum. Table 6 summarises the studies of WEC geometry optimisation which adopt exhaustive search or perform parametric studies, showing application to a broad range of WEC concepts.

Exhaustive search methods can consider nonlinear WEC hydrodynamics and control/PTO constraints. In Table 6, fully nonlinear WEC hydrodynamics are implicitly included in CFD or experimental methods, e.g. [114,117,121,122,124,134–137,144,150]. Fully nonlinear potential flow theory is applied in [115] via a package called HOBEM, to consider the effects of large waves. Hybrid modelling methods are applied in [145,194] with viscosity treatment, while the viscosity effect is linearised as a linear damping term in [99]. Control constraints can also be handled easily using exhaustive search methods. For instance, constraints on velocity and displacement are considered in [33,70,83,105,146,194], and PTO force constraints are considered in [33]. In addition, constraints on hydrodynamic WEC loads on the body can also be accounted for, via slamming restrictions in [83,102].

When the number or space of the design parameters increase, exhaustive search or parametric studies methods may become computationally intractable and more sophisticated search methods are required to accelerate the optimisation procedure, such as local or global search methods, detailed in the following subsections.

### 9.2. Local search methods

Local search methods include gradient-based and direct search methods. As the cost function  $F(\mathbf{X})$  in Eq. (56) is rarely expressible in algebraic form, analytic gradients cannot be evaluated, with a need to resort to less accurate numerical gradients. Some gradient-based methods have been applied inside WEC geometric optimisation loops to determine the optimal PTO damping coefficient, e.g. [107,125]. In addition, the gradient-based Fletcher–Reeves algorithm is used to optimise the inner pendulum (working as a PTO) design for the SEAREV devices for each iteration of its hull optimisation [96,103]. These gradient-based algorithms are not dwelt on here, since they are only used to find optimal PTO setups for WEC geometric optimisation. Some direct search methods applied for WEC geometric optimisation are summarised in Table 7, including the constrained optimisation by linear approximation (COBYLA) [125–128] and the simple pattern search method [130].

In Table 7, the viscous effect articulated in Eq. (32) is considered in [79], but linearised as a equivalent damper in the spectral domain. A comparison study between the COBYLA and differential evolution (DE) method is conducted in [125], concluding that the DE algorithm has the advantage of a high probability of convergence to a global optimum. However, it requires a much higher number of evaluating the cost function, which results in significantly longer computational time. In addition, only slight differences are found in the optimised results

**Table 6**

Overview of geometric optimisation of WEC systems by exhaustive search or parametric study methods. Abbreviations: surge (S), heave (H), pitch (P), time domain (TD), frequency domain (FD), regular wave (RW), irregular wave (IW), wave climate (WC), reactive control (RC), passive control (PC), latching control (LC), declutching control (DC), and pseudo-spectral optimal control (PSOC).

WEC type	Shapes	Modes	Hydrodynamic modelling	Domains	Wave conditions	Control approaches	Performance criteria	References
PA	Cyl	H	Experimental WAMIT	TD FD	IW WC	DC LC RC PSOC	$P_v$ $P_a$ RAO	[33,64,71]
PA	Cyl	S, H, P	Analytical	FD	IW	RC	RAO	[70]
PA	Cyl CylCon Sph CylSph	H	AQWA	FD	WC	PC	$P_a$	[73]
PA	Cyl, Sph ConCylCon	H	WAMIT	TD	IW RW	RC LC	$P_v$ CWR	[78]
PA	CylCon	H	AQUA+ Experimental	TD	RW IW	PC	$P_a$ , CWR RAO	[82,84]
PA	CylCon CylSph	H	WAMIT AQWA	TD	IW	RC	$P_a$ CWR	[83,85,87]
PA	Cyl-Plt Cyl-Sph	H	AQWA WAMIT WEC-Sim	TD	RW IW	PC RC	$P_a$	[99,101]
PA	Hul-Pdl	H	Hybrid	TD	RW WC	PC	RAO, CWR	[105]
PA	Sph-Sph	H	Analytical	FD	WC	PC	AEP, LCoE	[102]
OWC	UnivFix	-	Analytical Empirical OpenFOAM	FD TD	RW IW	PC	RAO CWR	[108-110,172]
OWC	FrntShp	-	CFX, FLOW3D Experimental	TD	RW IW	PC	CWR	[116,117]
OWC	BtmShp	-	HOBEM Experimental	TD	RW	PC	CWR	[112,115]
OWC	BtmShp	-	CFX	TD	RW	PC	RAO	[114]
OWC	U-shape	-	HOBEM	TD	RW	PC	CWR	[119]
OWC	UnivFlt	-	FLUENT	TD	RW	-	$P_a$	[121,124]
OWC	UnivFlt	-	STAR-CCM+	TD	RW	-	CWR	[122]
OWC	UnivFlt	-	Analytical	FD	RW	PC	CWR	[123]
OWC	Spar-buoy	-	WAMIT	FD	RW, IW	RC	EP, $P_a$	[124]
OWC	BBDB	-	WAMIT	FD	RW	PC	CWR	[127]
AWEC	Barge	P	WAMIT	TD	RW IW, WC	PC	$P_a$	[131]
TWEC	Flap-vane	P	Hybrid	FD	RW	PC	$P_a$	[28-30]
TWEC	Duck	P	AQWA	FD	RW	RC	CWR	[133]
TWEC	Cylinder	P	Analytical	TD	RW	RC	CWR	[145]
TWEC	Flap	P	Analytical	FD	RW	PC	CWR	[148]
TWEC	Flap	P	Hybrid	FD	RW	LC	CWR, $P_v$	[194]
TWEC	Cylinder	P	Experimental	TD	RW, IW	PC	CWR	[146]
TWEC	C-cell	P	OpenFOAM	TD	RW	PC	$P_a$ , CWR	[150]
TWEC	SSG	-	NEMOH Empirical Experimental	TD	IW, WC RW, IW	PC	CWR	[141-143]
TWEC	WD	-	Empirical Experimental	TD	RW IW	-	CWR	[134-136,144]
TWEC	WD	-	FLUENT	TD	RW	-	CWR	[137]
TWEC	WaveCat	-	Experimental	TD	IW	-	$P_a$ , CWR	[138,140]

**Table 7**

Overview of geometric optimisation of WEC systems by local search methods. Abbreviations: pitch (P), frequency domain (FD), regular wave (RW), wave climate (WC), reactive control (RC), passive control (PC) and constrained optimisation by linear approximation (COBYLA).

WEC type	Shapes	Modes	Modelling	Domains	Wave conditions	Control approaches	Optimisation criteria	Methods	References
OWC	Spar-buoy	-	WAMIT	FD	WC	PC	CWR	COBYLA	[125,126]
OWC	BBDB	-	WAMIT	FD	WC	PC	CWR LCoE	COBYLA	[127]
OWC	UGEN	-	WAMIT	FD	WC	PC	CWR	COBYLA	[128]
AWEC	Barge	P	WAMIT	FD	RW	RC	$P_a$ , NPV	Pattern search	[130]

returned by the two methods, less than 1% in term of mean annual power for all wave conditions. One extension of basic line searches to counter multi-modal performance surfaces is to use multiple initial conditions, which may be computationally more economical than full parallel search. For example, for the geometric optimisation of a barge-type AWEC device [130], searching with multiple starts is effective to find the global optimal solution. Such an approach has also been employed in aerodynamic optimisation [258].

### 9.3. Global search methods

Compared to local search methods, global search methods can increase the likelihood of finding the global optimal solution, but generally require significantly more computational resources. In general, global search methods vary from case to case, and heuristic algorithms, especially evolutionary algorithms (EAs), have demonstrated their capability in offering robust methods to find a global optimum

without requiring the information of derivatives or continuity of cost functions [258].

### 9.3.1. Evolutionary algorithms

Evolutionary algorithms are generally used for a broad range of engineering applications, and include genetic algorithms (GAs), evolutionary strategies, particle swarm optimisation (PSO), differential evolution (DE), etc. A comparison study of GA, PSO and DE is conducted in [261], which concludes that the key difference of these algorithms lies in how to generate the new population in each iteration with different balances between intensification and diversification.

Among these EAs, GAs are the most popular and well-established methods, and Table 8 summarises the application of GAs for hydrodynamic optimisation of WEC devices. GAs do not require a cost function gradient, and have less dependence on the continuity of the design space. Hence, GAs can be applied to a wide variety of WEC concepts. In addition, control constraints in terms of power and motion [151,152], and time-varying mass and damping coefficients of the water column in a U-OWC [118], can also be considered. A detailed description of GAs are given in [262,263].

Other evolutionary algorithms used for WEC geometric optimisation are summarised in Table 9. A simple evolutionary algorithm (1+1EA), covariance matrix adaptation evolution strategy (CMAES), differential evolution (DE), self-adaptive differential evolution (SaDE) and particle swarm optimisation (PSO) are compared in [79]. Multiple objective evolutionary algorithms (MOEAs) are adopted for hydrodynamic optimisation of PAs and AWECs in [59,147].

### 9.3.2. Other global search algorithms

In addition to evolutionary algorithms, a variety of global search methods exist, but only a few are applied for WEC hydrodynamic optimisation, including the Nelder–Mead simplex method (NMSM), the response surface method (RSM) and the Taguchi method, as summarised in Table 10. Additionally, the viscous effect is considered as a linearised equivalent damper in [100].

### 9.4. Influence of optimisation algorithm on optimal geometry

In general, the selection of local or global search methods may have only a slight influence on the optimised geometry, but displays a dramatic difference in computation time. A comparison study between the COBYLA and the DE methods is discussed in [125]. In this study, only slight differences are found in the optimised results by the two methods, less than 1% in term of mean annual power for all testing cases. However, the DE has the advantage of a high probability of convergence to a global optimum, but also requires a much higher number of cost evaluations to converge, which results in correspondingly higher computational time. By way of example, an Intel Core i7 CPU @ 2.8 GHz is used in [125], where the COBYLA method required approximately 10 h computation, while the DE method required approximately 903 h. Similar conclusions have been drawn in aerodynamic optimisation [258].

The choice of optimisation algorithm will undoubtedly affect the optimisation results to some extent. A variety of optimisation algorithms are compared in [79], including the 1+1EA, NMSM, CMAES, DE, PSO and SaDE methods. In this study, the optimised radii by the aforementioned algorithms vary in the range of  $r \in [18, 19.8]$  when the mean annual power is used as the cost function, while the radii are  $r \in [12.2, 14.7]$  when the LCoE (simplified as  $LCoE = AEP_m^{-0.5}$ ) is used as the cost function. Compared to the influence of the choice of a particular optimisation algorithm, the selection of a performance criterion has much more significant influence on the optimised geometry. Also, a hybrid method, i.e. the DE-NMSM method, is tried in [79], but no specific comparison is made against other algorithms.

Finally, the interplay between the complexity of the optimisation problem (reflecting the geometry and number of parameters to be

optimised) and the performance function employed may have a significant bearing on the convexity of the resulting optimisation problem. This may have a significant influence on the appropriate choice of optimisation algorithm, with the methods described in Section 9.2 being potentially ineffective in determining the global optimum for a significantly multi-modal performance surface. Equally, though the methods of Section 9.1 provide exhaustive performance function computation of all optimisation parameter combinations, and therefore will generally reveal the global optimum (subject to the level of grid resolution), the computational cost may be excessive. Therefore, some insight into the nature of the optimisation problem is crucial if an appropriate optimisation algorithm is to be chosen.

## 10. Discussion

Based on the references in Tables 1–10, pie charts are presented in Fig. 12, to summarise the diversity of WEC hydrodynamic optimisation efforts in terms of WEC concepts, wave conditions, modelling methods, control strategies, optimisation criteria, and optimisation algorithms, detailed as follows:

- It can be seen from Fig. 12(a) that PA concepts are most popular, with 63% of studies on hydrodynamic optimisation, of which 50% are for single-body, and 13% for two-body, PAs. The OWC and TWEC concepts are evenly divided with a 17% share each, but only 3% studies focus on the AWEC concepts. These findings show a high consistency with the statistical results given in [14].
- As shown in Fig. 12(b), regular and irregular wave conditions are evenly applied for WEC hydrodynamic optimisation. Within the studies using irregular waves, 15% consider wave climates to obtain more applicable shapes for specific wave farms.
- Another basis for comparison is the selection of hydrodynamic modelling methods. As illustrated in Fig. 12(c), most modelling methods are in the time and frequency domains, with only 4% studies in the spectral domain. The potential flow theory, including the FNPF, LPF and analytical methods, is generally used to model the WSI. Up to 10% of studies use hybrid modelling methods, but mainly consider the viscous effect as a linearised equivalent damper. Fully nonlinear WSI are considered implicitly when experimental or CFD methods are used. However, these methods are expensive in cost or computation. In addition, the layout of wave farm or WEC arrays can also affect the optimised geometry of a component device [48,68], and the interaction between WECs should be considered. Clearly, for model-based optimisation to be meaningful, the mathematical/computational model employed should be validated, as discussed in Section 4.
- Control strategies are critical for maximising power output of WEC systems, and most geometric optimisation studies apply classical control methods, e.g. reactive control 25%, passive control 66%, and latching or declutching control 5%. Only 4% of studies consider modern control strategies, e.g. the pseudo spectral optimal control. However, control strategies tend to exaggerate WEC motion, and consequently result in strong nonlinearity in the WSI. Thus, hydrodynamic optimisation should consider both modern control strategies and so-induced nonlinear effects in hydrodynamic modelling. In addition, PTO systems for control actuation are assumed ideal, and the influence of non-ideal PTOs on WEC geometric optimisation is unknown. This also suggests a co-design framework for WEC hydrodynamic optimisation.
- For advancing commercial applications, WEC geometric optimisation should aim to minimise the LCoE or maximise the NPV. However, only 8% of studies try to optimise WEC designs based on economic criteria (see Fig. 12(e)). In contrast, the majority, up to 78% of studies, aim to maximise technical criteria, e.g. the average power absorption, annual energy production, capture width ratio and RAO, mainly due to more straightforward performance



**Table 8**

Overview of geometric optimisation of WEC systems by genetic algorithms. Abbreviations: surge (S), heave (H), pitch (P), time domain (TD), frequency domain (FD), spectral domain (SD), regular wave (RW), irregular wave (IW), wave climate (WC), reactive control (RC), passive control (PC) and pseudo spectral optimal control (PSOC).

WEC type	Shape	Modes	Hydrodynamic modelling	Domain	Wave conditions	Control approaches	Performance criteria	References
PA	ArbShp	H	NEMOH	TD	IW	PSOC	$P_a$	[60]
PA	ArbShp	H	NEMOH	TD	WC	RC	$P_a$	[62]
PA	ArbShp	S, H, P	WAMIT	FD, TD	IW	PC	$P_a, P_v, P_s$	[92,94,95]
PA	Hul-Pdl	P	AQUA+	TD	WC	PC	$P_a$	[96,103]
PA	Hul-Pdl	H	NEMOH	FD	IW	RC	Cost of power, $CWR$	[106]
PA	Hul-Pdl	P, S	ACHIL3D	TD	WC	PC	$AEP$	[104]
PA	Cyl-Pst	H	WAMIT	FD	RW, WC	RC	$P_v$	[107]
OWC	U-shape	-	Analytical	SD	IW	PC	$P_a$	[118]
OWC	UGEN	-	WAMIT	FD	WC	PC	$P_a$	[128]
TWEC	Flap	P	Analytical	FD	IW	PC	$CWR$	[149]
TWEC	ArbShp	P	WAMIT	FD	RW, IW	RC	Power per length, $P_v$	[151,152]

**Table 9**

Overview of geometric optimisation of WEC systems by other evolutionary algorithms (excluding GAs). Abbreviations: heave (H), surge (S), frequency domain (FD), spectral domain (SD), regular wave (RW), irregular wave (IW), wave climate (WC), reactive control (RC) and passive control (PC).

WEC type	Shapes	Modes	Modelling methods	Domains	Wave conditions	Control	Optimisation criteria	Methods	References
PA	ArbShp	H, S	WAMIT	FD	IW	PC	$P_a$	MOEA	[59]
PA	ArbShp	H, S, P	WAMIT	TD	IW	PC	$P_a, P_v, P_s$	PSO	[95]
PA	Cyl	6 DoFs	Hybrid	SD	WC	RC	$P_a$ $LCoE$	1+1EA, DE CMAES PSO, SaDE	[79]
OWC	Spar-buoy	-	WAMIT	FD	WC	PC	$CWR$	DE	[125]
AWEC	Flap, C-cell	S	WAMIT	FD	RW	RC	Force per power Area per power	MOEA	[147]

**Table 10**

Overview of geometric optimisation of WEC systems by other global search methods. Abbreviations: heave (H), pitch (P), time domain (TD), frequency domain (FD), spectral domain (SD), regular wave (RW), irregular wave (IW), wave climate (WC), reactive control (RC), passive control (PC), Nelder–Mead simplex method (NMSM), particle swarm optimisation (PSO) and response surface method (RSM).

WEC type	Shapes	Modes	Modelling methods	Domains	Wave conditions	Control approaches	Optimisation criteria	Methods	References
PA	Cyl	H	ACHIL3D	TD	IW	PC, LC	$P_a$	NMSM	[53]
PA	Cyl	6 DoFs	Hybrid	SD	IW	RC	$P_a, LCoE$	NMSM	[79]
PA	Cyl	H, P	AQWA	TD	RW	PC	$P_a$	RSM	[63]
PA	Cyl–Cyl, Cyl–Sph	H	Hybrid	FD	RW	PC	Cost of material $P_a$	Taguchi	[100]
AWEC	Seaweed	P	WAMIT	FD	RW, WC	PC	$P_a, CWR$	RSM	[132]

function evaluation. Some studies try to balance economic and technical criteria by using a techno-economic criterion, e.g. power per surface/volume/mass, AEP per surface/volume/mass.

- The optimisation problem of WEC geometry is somewhat opaque, with numerical hydrodynamic calculations (among other issues) obscuring the relationship between geometric parameters and the performance function. As a result, the (possible multi-modal) nature of the optimisation problem is very poorly defined, with exhaustive search methods often applied, with a percentage up to 63%, as shown in Fig. 12(f). Clearly, there is ample scope to improve understanding of the nature of the geometry optimisation problem, if appropriate, efficient, and capable optimisation algorithms are to be identified and employed.

The development of the SEAREV device, summarised in [256], is a good reference case study for WEC hydrodynamic optimisation. Three generations of prototype shapes are optimised, with the first generation aiming to simultaneously maximise annual power absorption and minimise the displaced mass, the second round aiming to reduce nonlinear slamming and parametric resonance, and the third stage aiming to optimise detailed mechanical design. A noteworthy finding from this case study is that a higher TPL for WEC concepts is required, and the TPL should be considered at the very beginning of WEC projects, showing consistency with the findings in [4,37,38].

**11. Conclusions**

This review summaries the state-of-the-art of WEC geometric optimisation, with the main findings concluded as follows:

- WEC concepts, including operational modes and geometry definitions, have a significant influence on the optimised geometries. However, there is no solid evidence to any concept over others. This suggests the need for benchmarking studies, and explains the lack of convergence in the development of WEC concepts.
- Wave conditions have a significant influence on WEC geometric optimisation, and for a specific project, annual wave climate is recommended as input data for optimisation. This can help to customise a device to a specific location, but may result in a significant computational burden. However, it is likely to display the diversity in geometry for a particular site customisation.
- It is clear that hydrodynamic modelling methods play an import role in WSI and, given the sensitivity of WEC dynamics to power maximisation control (potentially exaggerating nonlinear effects), no clear results are yet available on the sensitivity of optimal geometry to the nature of the hydrodynamic model employed. This could be an important area for further research. Equally, as articulated in Section 4, it is important that the hydrodynamic models, at least in their generic form, are representative and, to some extent validated against experimental data.
- Different control strategies have a significant influence on the optimised dimensions of WEC geometry. Optimised WEC shapes are sensitive to control constraints, e.g. displacement, force and power constraints. The energy transfer efficiency of PTO units is generally assumed ideal, and non-ideal PTO, considering mechanical, hydraulic or/and electrical losses, are not normally considered. Questions still remain as to how non-ideal PTO modelling affects WEC optimised geometry.

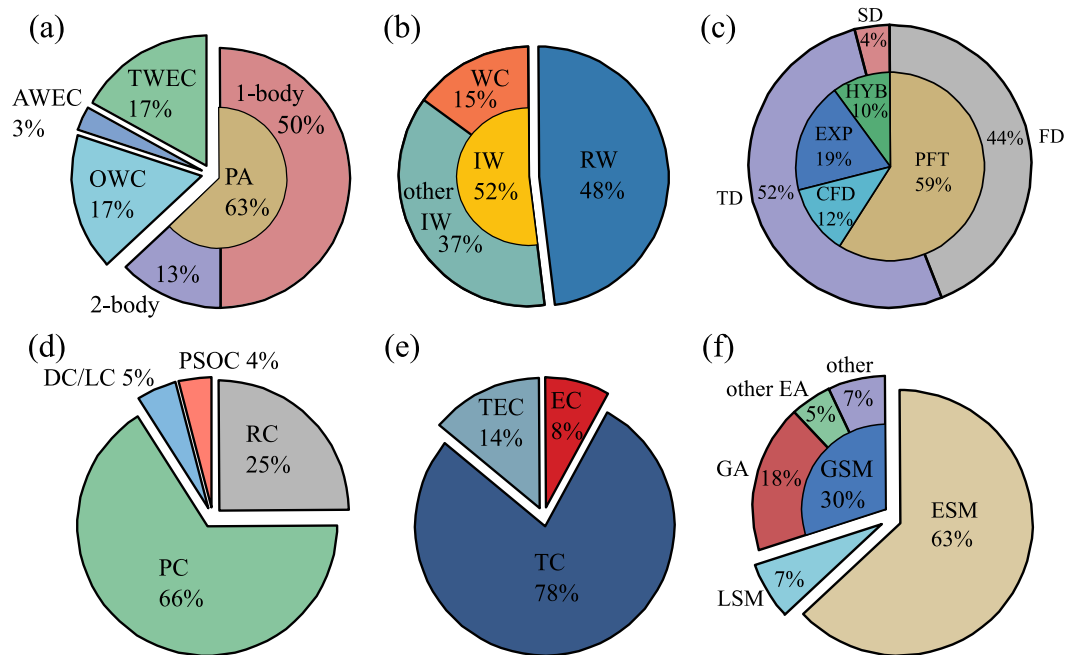


Fig. 12. Pie charts showing percentages of WEC concepts (a), wave conditions (b), hydrodynamic modelling methods (c), control strategies (d), optimisation criteria (e) and optimisation algorithms (f). Abbreviations: point absorber (PA), oscillating water column (OWC), attenuator-type wave energy converter (AWEC), terminator-type wave energy converter (TWEC), regular wave (RW), irregular wave (IW), wave climate (WC), frequency domain (FD), time domain (TD), spectral domain (SD), potential flow theory (PFT), computational fluid dynamics (CFD), experimental (EXP), hybrid (HYB), reactive control (RC), passive control (PC), latching control (LC), declutching control (DC), pseudo spectral optimal control (PSOC), economic criteria (EC), technical criteria (TC), techno-economic criteria (TEC), exhaustive search method (ESM), local search method (LSM), global search method (GSM), genetic algorithm (GA) and evolutionary algorithm (EA).

- Optimisation criteria have dramatic influence on WEC hydrodynamic optimisation; economic-driven, techno-economic and technical criteria tend to result in small, median and large shapes, respectively. However, it is still difficult to evaluate economic criteria, e.g. LCoE and NPV, as a cost function in the optimisation procedure, since a high level uncertainty exists in estimating these criteria. This uncertainty may be alleviated by the increasing operation experience of WEC farms. However, ultimately, the most meaningful performance indicators are those based exclusively on economic metrics, providing they consider all technical limitations and characteristics.
- Compared to other factors, optimisation algorithm has a relatively limited influence on WEC geometric optimisation, though this depends on the degree of multi-modality in the performance surface, which is likely to some extent, given that the optimisation problem is multi-parameter, multi-objective and implicit.

WEC geometry optimisation should be an indispensable procedure at the initial stages of any WEC project to evaluate its technical, and ideally economic, performance over the whole life-cycle. As concluded from some sea trials of WEC systems, it is important to prioritise TPL over TRL, especially at initial to mid-term stages of development. In addition, a systematic co-design framework is still missing for WEC hydrodynamic optimisation. Such a co-design framework should be capable of covering all the main factors which can significantly influence the optimisation results, including wave climates, flexible geometry definition, nonlinear WSI, control strategies, non-ideal PTO systems, economic or techno-economic criteria, and tailored optimisation algorithms. While many of these issues have been covered individually, or in partial combination, to date no concerted approach has been taken, potentially invalidating many of the conclusions drawn to date.

#### Declaration of competing interest

The authors declare that they have no known competing financial interests or personal relationships that could have appeared to influence the work reported in this paper.

#### References

- [1] Clément A, McCullen P, Falcão A, Fiorentino A, Gardner F, Hammarlund K, et al. Wave energy in Europe: Current status and perspectives. *Renew Sustain Energy Rev* 2002;6(5):405–31.
- [2] McCormick ME. *Ocean wave energy conversion*. New York: Wiley; 1981.
- [3] Gunn K, Stock-Williams C. Quantifying the global wave power resource. *Renew Energy* 2012;44:296–304.
- [4] Weber J, Costello R, Ringwood J. WEC technology performance levels (TPLs)-metric for successful development of economic WEC technology. In: Proc. European wave and tidal energy conference. Aalborg, Denmark: 2013.
- [5] Folley M, Babarit A, Child B, Forehand D, Boyle LO, Silverthorne K, et al. A review of numerical modelling of wave energy converter arrays. In: Proc. international conference on ocean, offshore and arctic engineering. Rio de Janeiro, Brazil: 2012. p. 535–45.
- [6] Penalba M, Giorgi G, Ringwood JV. Mathematical modelling of wave energy converters: A review of nonlinear approaches. *Renew Sustain Energy Rev* 2017;78:1188–207.
- [7] Windt C, Davidson J, Ringwood JV. High-fidelity numerical modelling of ocean wave energy systems: A review of computational fluid dynamics-based numerical wave tanks. *Renew Sustain Energy Rev* 2018;93:610–30.
- [8] Sheng W. Wave energy conversion and hydrodynamics modelling technologies: A review. *Renew Sustain Energy Rev* 2019;109:482–98.
- [9] Ringwood JV, Bacelli G, Fusco F. Energy-maximizing control of wave-energy converters: The development of control system technology to optimize their operation. *IEEE Control Syst Mag* 2014;34(5):30–55.
- [10] Faedo N, Olaya S, Ringwood JV. Optimal control, MPC and MPC-like algorithms for wave energy systems: An overview. *IFAC J Syst Control* 2017;1:37–56.
- [11] Wang L, Isberg J, Tedeschi E. Review of control strategies for wave energy conversion systems and their validation: The wave-to-wire approach. *Renew Sustain Energy Rev* 2018;81:366–79.
- [12] Ringwood JV. Wave energy control: Status and perspectives 2020. In: Proc. IFAC world congress. Berlin, Germany: 2020. p. 1–12.
- [13] Bard J, Kracht P. Report on linear generator systems for wave energy converters. Tech. rep., Fraunhofer IWES; 2013.
- [14] López I, Andreu J, Ceballos S, De Alegría IM, Kortabarria I. Review of wave energy technologies and the necessary power-equipment. *Renew Sustain Energy Rev* 2013;27:413–34.
- [15] Chiba S, Waki M, Wada T, Hirakawa Y, Masuda K, Ikoma T. Consistent ocean wave harvesting using electroactive polymer (dielectric elastomer) artificial muscle generators. *Appl Energy* 2013;104:497–502.
- [16] Polinder H, Damen ME, Gardner F. Linear PM generator system for wave energy conversion in the AWS. *IEEE Trans Energy Convers* 2004;19(3):583–9.

- [17] Lin Y, Bao J, Liu H, Li W, Tu L, Zhang D. Review of hydraulic transmission technologies for wave power generation. *Renew Sustain Energy Rev* 2015;50:194–203.
- [18] Falcão AF, Henriques JC. Oscillating-water-column wave energy converters and air turbines: A review. *Renew Energy* 2016;85:1391–424.
- [19] Ahamed R, McKee K, Howard I. Advancements of wave energy converters based on power take off (PTO) systems: A review. *Ocean Eng* 2020;204:107248.
- [20] Boake CB, Whittaker TJ, Folley M, Ellen H, et al. Overview and initial operational experience of the LIMPET wave energy plant. In: Proc. international offshore and polar engineering conference. Kitakyushu, Japan: 2002. p. 586–94.
- [21] Falcão AF, Sarmento AJ, Gato LM, Brito-Melo A. The Pico OWC wave power plant: Its lifetime from conception to closure 1986–2018. *Appl Ocean Res* 2020;98:102104.
- [22] Ibarra-Berastegi G, Sáenz J, Ulazia A, Serras P, Esnaola G, Garcia-Soto C. Electricity production, capacity factor, and plant efficiency index at the Mutriku wave farm (2014–2016). *Ocean Eng* 2018;147:20–9.
- [23] Yemm R, Pizer D, Retzler C, Henderson R. Pelamis: Experience from concept to connection. *Phil Trans R Soc A* 2012;370(1959):365–80.
- [24] Whittaker T, Folley M. Nearshore oscillating wave surge converters and the development of oyster. *Phil Trans R Soc A* 2012;370(1959):345–64.
- [25] Kofoed JP, Frigaard P, Friis-Madsen E, Sørensen HC. Prototype testing of the wave energy converter wave dragon. *Renew Energy* 2006;31(2):181–9.
- [26] Sjolte J, Bjerke I, Tjensvoll G, Molinas M. Summary of performance after one year of operation with the lifesaver wave energy converter system. In: Proc. European wave and tidal energy conference. Aalborg, Denmark: 2013.
- [27] Astariz S, Iglesias G. The economics of wave energy: A review. *Renew Sustain Energy Rev* 2015;45:397–408.
- [28] Papillon L, Wang L, Tom N, Weber J, Ringwood J. Parametric modelling of a reconfigurable wave energy device. *Ocean Eng* 2019;186:106105.
- [29] Tom N, Lawson M, Yu Y-h, Wright A. Preliminary analysis of an oscillating surge wave energy converter with controlled geometry. In: Proc. European wave and tidal energy conference. Nantes, France: 2015.
- [30] Tom NM, Lawson MJ, Yu YH, Wright AD. Development of a nearshore oscillating surge wave energy converter with variable geometry. *Renew Energy* 2016;96:410–24.
- [31] Rhinefrank K, Schacher A, Prudell J, Brekken TK, Stillinger C, Yen JZ, et al. Comparison of direct-drive power takeoff systems for ocean wave energy applications. *IEEE J Ocean Eng* 2011;37(1):35–44.
- [32] Liang C, Ai J, Zuo L. Design, fabrication, simulation and testing of an ocean wave energy converter with mechanical motion rectifier. *Ocean Eng* 2017;136:190–200.
- [33] Garcia-Rosa PB, Bacelli G, Ringwood JV. Control-informed geometric optimization of wave energy converters: The impact of device motion and force constraints. *Energies* 2015;8(12):13672–87.
- [34] Guo B, Ringwood JV. Modelling of a vibro-impact power take-off mechanism for wave energy conversion. In: Proc. European control conference. Saint Petersburg, Russia: 2020. p. 1348–53.
- [35] Guo B, Ringwood JV. Non-linear modelling of a vibro-impact wave energy converter. *IEEE Trans Sustain Energy* 2021;12:492–500.
- [36] Ekström R, Ekergård B, Leijon M. Electrical damping of linear generators for wave energy converters—A review. *Renew Sustain Energy Rev* 2015;42:116–28.
- [37] Weber JW, Laird D, Costello R, Roberts J, Bull D, Babarit A, et al. Cost, time, and risk assessment of different wave energy converter technology development trajectories. In: Proc. European wave and tidal energy conference. Cork, Ireland: 2017.
- [38] Weber J, Teillant B, Costello R, Ringwood J, Soulard T. Integrated WEC system optimisation—Achieving balanced technology development and economical lifecycle performance. In: Proc. European wave and tidal energy conference. Southampton, UK: 2011.
- [39] Clark CE, Garcia-Teruel A, DuPont B, Forehand D. Towards reliability-based geometry optimization of a point-absorber with PTO reliability objectives. In: Proc. European wave and tidal energy conference. Napoli, Italy: 2019.
- [40] Balitsky P, Bacelli G, Ringwood JV. Control-influenced layout optimization of arrays of wave energy converters. In: Proc. international conference on ocean, offshore and arctic engineering. San Francisco, USA: 2014. p. 1–10.
- [41] Child BFM. On the configuration of arrays of floating wave energy converters [Ph.D. thesis], University of Edinburgh; 2011.
- [42] Fang HW, Feng YZ, Li GP. Optimization of wave energy converter arrays by an improved differential evolution algorithm. *Energies* 2018;11(3522):1–19.
- [43] Garcia-Rosa PB, Bacelli G, Ringwood JV. Control-informed optimal array layout for wave farms. *IEEE Trans Sustain Energy* 2015;6(2):575–82.
- [44] Giassi M, Göteman M. Layout design of wave energy parks by a genetic algorithm. *Ocean Eng* 2018;154:252–61.
- [45] Lyu J, Abdelkhalik O, Gauchia L. Optimization of dimensions and layout of an array of wave energy converters. *Ocean Eng* 2019;192:106543.
- [46] McGuinness JP, Thomas G. Hydrodynamic optimisation of small arrays of heaving point absorbers. *J Ocean Eng Mar Energy* 2016;2(4):439–57.
- [47] Ruiz PM, Nava V, Topper MB, Minguela PR, Ferri F, Kofoed JP. Layout optimisation of wave energy converter arrays. *Energies* 2017;10(9):1–17.
- [48] Penalba M, Touzón I, Lopez-Mendia J, Nava V. A numerical study on the hydrodynamic impact of device slenderness and array size in wave energy farms in realistic wave climates. *Ocean Eng* 2017;142:224–32.
- [49] Sarkar D, Contal E, Vayatis N, Dias F. Prediction and optimization of wave energy converter arrays using a machine learning approach. *Renew Energy* 2016;97:504–17.
- [50] Neshat M, Alexander B, Wagner M. A hybrid cooperative co-evolution algorithm framework for optimising power take off and placements of wave energy converters. *Inform Sci* 2020;534:218–44.
- [51] Giorgi G, Penalba M, Ringwood JV. Nonlinear hydrodynamic models for heaving buoy wave energy converters. In: Proc. Asian wave and tidal energy conference. Marina Bay Sands, Singapore: 2016. p. 1–10.
- [52] Korde UA, Ringwood J. Hydrodynamic control of wave energy devices. Cambridge University Press; 2016.
- [53] Gilloteaux JC, Ringwood J. Control-informed geometric optimisation of wave energy converters. In: Proc. IFAC conference on control applications in marine systems. Rockstock, Germany: 2010. p. 366–71.
- [54] Sergiienko NY. Three-tether wave energy converter: hydrodynamic modelling, performance assessment and control [Ph.D. thesis], University of Adelaide; 2018.
- [55] Thorpe TW. A brief review of wave energy: a report produced for UK Department of Trade and Industry. Tech. rep., AEA Technology; 1999, Report No ETSU-120.
- [56] Drew B, Plummer A, Sahinkaya M. A review of wave energy converter technology. *Proc Inst Mech Eng A* 2009;223(8):887–902.
- [57] Falcão AF. Wave energy utilization: A review of the technologies. *Renew Sustain Energy Rev* 2010;14(3):899–918.
- [58] Guo B, Patton R, Abdelrahman M, Lan J. A continuous control approach to point absorber wave energy conversion. In: UKACC international conference on control. Belfast, UK: IEEE; 2016. p. 1–6.
- [59] Gunn KJ, Lingwood CJ, Taylor CJ. Multi-objective evolutionary optimisation of the geometry of a class of controlled wave energy converter. In: Proc. UKACC international conference on control. Coventry, UK: 2010. p. 349–54.
- [60] Abdelkhalik O, Coe R, Bacelli G, Wilson DG. WEC geometry optimisation with advanced control. In: Proc. international conference on ocean, offshore and arctic engineering. Trondheim, Norway: 2017. p. 1–8.
- [61] McTiernan K. A heuristic optimization approach to hydrodynamic wave energy converter geometry [Ph.D. thesis], University of Washington; 2018.
- [62] Esmaeilzadeh S, Alam MR. Shape optimization of wave energy converters for broadband directional incident waves. *Ocean Eng* 2019;174:186–200.
- [63] Koh HJ, Ruy WS, Cho IH, Kweon HM. Multi-objective optimum design of a buoy for the resonant-type wave energy converter. *J Mar Sci Technol* 2015;20(1):53–63.
- [64] Garcia-Rosa PB, Ringwood JV. On the sensitivity of optimal wave energy device geometry to the energy maximizing control system. *IEEE Trans Sustain Energy* 2016;7(1):419–26.
- [65] Zhang W, Liu H, Zhang L, Zhang X. Hydrodynamic analysis and shape optimization for vertical axisymmetric wave energy converters. *China Ocean Eng* 2016;30(6):954–66.
- [66] Rafee A, Fiévez J. Numerical prediction of extreme loads on the CETO wave energy converter. In: Proc. European wave and tidal energy conference. Nantes, France: 2015.
- [67] Jin S, Patton R. Geometry influences on hydrodynamic responses of a heaving point absorber wave energy converter. In: Proc. European wave and tidal energy conference. Cork, Ireland: 2017.
- [68] Göteman M. Wave energy parks with point-absorbers of different dimensions. *J Fluids Struct* 2017;74:142–57.
- [69] Alves A, Sarmento A. Hydrodynamic optimization of the active surface of a heaving point absorber WEC. In: Proc. European wave and tidal energy conference. Uppsala, Sweden: 2009. p. 610–17.
- [70] Bachynski EE, Young YL, Yeung RW. Analysis and optimization of a tethered wave energy converter in irregular waves. *Renew Energy* 2012;48:133–45.
- [71] Sjökvist L, Krishna R, Rahm M, Castellucci V, Hagnestål A, Leijon M. On the optimization of point absorber buoys. *J Mar Sci Eng* 2014;2(2):477–92.
- [72] Chen Z, Zhou B, Zhang L, Zhang W, Wang S, Zang J. Geometrical evaluation on the viscous effect of point-absorber wave-energy converters. *China Ocean Eng* 2018;32(4):443–52.
- [73] Goggins J, Finnegan W. Shape optimisation of floating wave energy converters for a specified wave energy spectrum. *Renew Energy* 2014;71:208–20.
- [74] Zang Z, Zhang Q, Qi Y, Fu X. Hydrodynamic responses and efficiency analyses of a heaving-buoy wave energy converter with PTO damping in regular and irregular waves. *Renew Energy* 2018;116:527–42.
- [75] Shadman M, Estefan SF, Rodriguez CA, Nogueira IC. A geometrical optimization method applied to a heaving point absorber wave energy converter. *Renew Energy* 2018;115:533–46.
- [76] Jin S, Patton RJ, Guo B. Enhancement of wave energy absorption efficiency via geometry and power take-off damping tuning. *Energy* 2019;169:819–32.
- [77] Mavrakos SA, Katsaounis GM. Effects of floaters' hydrodynamics on the performance of tightly moored wave energy converters. *IET Renew Power Gener* 2010;4(6):531–44.



- [78] Sergiienko NY, Cazzolato BS, Ding B, Hardy P, Arjomandi M. Performance comparison of the floating and fully submerged quasi-point absorber wave energy converters. *Renew Energy* 2017;108:425–37.
- [79] Sergiienko NY, Neshat M, da Silva LSP, Alexander B, Wagner M. Design optimisation of a multi-mode wave energy converter. In: Proc. international conference on ocean, offshore and arctic engineering. Florida, USA: 2020.
- [80] Wilson DG, Robinett RD, Bacelli G, Abdelkhalik O, Weaver WW, Coe R. Nonlinear WEC optimized geometric buoy design for efficient reactive power requirements. In: Proc. oceans. Seattle, USA: 2019.
- [81] Wen Y, Wang W, Liu H, Mao L, Mi H, Wang W, et al. A shape optimization method of a specified point absorber wave energy converter for the South China Sea. *Energies* 2018;11(10):1–22.
- [82] Stallard TJ, Weller SD, Stansby PK. Limiting heave response of a wave energy device by draft adjustment with upper surface immersion. *Appl Ocean Res* 2009;31(4):282–9.
- [83] De Backer G, Vantorre M, Frigaard P, Beels C, De Rouck J. Bottom slamming on heaving point absorber wave energy devices. *J Mar Sci Technol* 2010;15(2):119–30.
- [84] Vantorre M, Banasiak R, Verhoeven R. Modelling of hydraulic performance and wave energy extraction by a point absorber in heave. *Appl Ocean Res* 2004;26(1–2):61–72.
- [85] Pastor J, Liu Y. Power absorption modeling and optimization of a point absorbing wave energy converter using numerical method. *J Energy Resour Technol* 2014;136(2):1–8.
- [86] Shi H, Han Z, Zhao C. Numerical study on the optimization design of the conical bottom heaving buoy converter. *Ocean Eng* 2019;173:235–43.
- [87] Berenjkoo MN, Ghiasi M, Soares CG. Influence of the shape of a buoy on the efficiency of its dual-motion wave energy conversion. *Energy* 2020. <http://dx.doi.org/10.1016/j.energy.2020.118998>.
- [88] Van de Sijpe A. Development of a point absorber wave energy converter: Realisation of power take-off, optimisation of geometry and installation techniques. Ghent University; 2012.
- [89] Ransley EJ, Greaves D, Raby A, Simmonds D, Hann M. Survivability of wave energy converters using CFD. *Renew Energy* 2017;109:235–47.
- [90] Alamian R, Shafaghat R, Bayani R, Amouei AH. An experimental evaluation of the effects of sea depth, wave energy converter's draft and position of centre of gravity on the performance of a point absorber wave energy converter. *J Mar Eng Technol* 2017;16(2):70–83.
- [91] Alamian R, Shafaghat R, Safaei MR. Multi-objective optimization of a pitch point absorber wave energy converter. *Water* 2019;11(5).
- [92] Garcia-Teruel A, Forehand D. Optimal wave energy converter geometry for different modes of motion. In: Proc. advances in renewable energies offshore. Lisbon, Portugal: 2018. p. 299–305.
- [93] Garcia-Teruel A, Forehand DJ, Jeffrey H. Metrics for wave energy converter hull geometry optimisation. In: Proc. European wave and tidal energy conference. Napoli, Italy: 2019. p. 1–6.
- [94] Garcia-Teruel A, Forehand D. Joint optimisation of geometry and mass distribution of wave energy converters. In: Proc. international conference on renewable energies offshore. Lisbon, Portugal: CRC Press; 2020. p. 81–8.
- [95] Garcia-Teruel A, DuPont B, Forehand DJ. Hull geometry optimisation of wave energy converters: On the choice of the optimisation algorithm and the geometry definition. *Appl Energy* 2020;280:115952. <http://dx.doi.org/10.1016/j.apenergy.2020.115952>.
- [96] Babarit A, Clement AH. Shape optimisation of the SEAREV wave energy converter. In: Proc. world renewable energy conference. Florence, Italy: 2006. p. 1–6.
- [97] Beatty SJ, Hall M, Buckham BJ, Wild P, Bocking B. Experimental and numerical comparisons of self-reacting point absorber wave energy converters in regular waves. *Ocean Eng* 2015;104:370–86.
- [98] Son D, Belissen V, Yeung RW. Performance validation and optimization of a dual coaxial-cylinder ocean-wave energy extractor. *Renew Energy* 2016;92:192–201.
- [99] Martin D, Wise A, Liang C, Zuo L. Shape optimization for the submerged body of a two-body wave energy converter. In: Proc. Europe wave tidal energy conference. 2017. p. 6.
- [100] Al Shami E, Wang X, Zhang R, Zuo L. A parameter study and optimization of two body wave energy converters. *Renew Energy* 2019;131:1–13.
- [101] Amiri A, Panahi R, Radfar S. Parametric study of two-body floating-point wave absorber. *J Mar Sci Appl* 2016;15(1):41–9.
- [102] Piscopo V, Benassai G, Cozzolino L, Della Morte R, Scamardella A. A new optimization procedure of heaving point absorber hydrodynamic performances. *Ocean Eng* 2016;116:242–59.
- [103] Clément A, Babarit A, Gilloteaux J-C, Josset C, Duclos G. The SEAREV wave energy converter. In: Proc. European wave and tidal energy conference. Glasgow, UK: 2005. p. 1–10.
- [104] Babarit A, Clément A, Ruer J, Tartivel C. SEAREV: A fully integrated wave energy converter. In: Proc. offshore wind and other marine renewable energies in Mediterranean and European Seas. Rome, Italy: 2006. p. 1–11.
- [105] Crowley S, Porter R, Taunton DJ, Wilson PA. Modelling of the WITT wave energy converter. *Renew Energy* 2018;115:159–74.
- [106] Sirigu SA, Foglietta L, Giorgi G, Bonfanti M, Cervelli G, Bracco G, et al. Techno-economic optimisation for a wave energy converter via genetic algorithm. *J Mar Sci Eng* 2020;8(482):1–29.
- [107] Gomes RP, Henriques JC, Gato LM, Falcão AF. IPS two-body wave energy converter: Acceleration tube optimization. *Int J Offshore Polar Eng* 2010;20(4):247–55.
- [108] Zheng S, Zhang Y, Iglesias G. Coast/breakwater-integrated OWC: A theoretical model. *Mar Struct* 2019;66:121–35.
- [109] He F, Zhang H, Zhao J, Zheng S, Iglesias G. Hydrodynamic performance of a pile-supported OWC breakwater: An analytical study. *Appl Ocean Res* 2019;88:326–40.
- [110] Simonetti I, Cappiotti L, El Safti H, Oumeraci H. Numerical modelling of fixed oscillating water column wave energy conversion devices: Toward geometry hydraulic optimization. In: Proc. international conference on ocean, offshore and arctic engineering. Newfoundland, Canada: 2015. p. 1–10.
- [111] Ulazia A, Esnaola G, Serras P, Penalba M. On the impact of long-term wave trends on the geometry optimisation of oscillating water column wave energy converters. *Energy* 2020;206:118146.
- [112] Ning DZ, Wang RQ, Zou QP, Teng B. An experimental investigation of hydrodynamics of a fixed OWC wave energy converter. *Appl Energy* 2016;168:636–48.
- [113] Ashlin SJ, Sundar V, Sannasiraj S. Effects of bottom profile of an oscillating water column device on its hydrodynamic characteristics. *Renew Energy* 2016;96:341–53.
- [114] Bouali B, Larbi S. Sequential optimization and performance prediction of an oscillating water column wave energy converter. *Ocean Eng* 2017;131:162–73.
- [115] Ning DZ, Ke S, Mayon R, Zhang C. Numerical investigation on hydrodynamic performance of an OWC wave energy device in the stepped bottom. *Front Energy Res* 2019;7:1–11.
- [116] Bouali B, Larbi S. Contribution to the geometry optimization of an oscillating water column wave energy converter. *Energy Procedia* 2013;36:565–73.
- [117] Mahnamfar F, Altunkaynak A. Comparison of numerical and experimental analyses for optimizing the geometry of OWC systems. *Ocean Eng* 2017;130:10–24.
- [118] Scialò A, Malara G, Arena F. Geometrical optimization of u-oscillating water columns in random waves. In: Proc. international conference on ocean, offshore and arctic engineering. Glasgow, Scotland: 2019. p. 1–8.
- [119] Ning D, Guo B, Wang R, Vyzikas T, Greaves D. Geometrical investigation of a U-shaped oscillating water column wave energy device. *Appl Ocean Res* 2020;97:102105.
- [120] Gomes MdN, Santos EDD, Isoldi LA, Rocha LAdO. Two-Dimensional geometric optimization of an oscillating water column converter of real scale. In: Proc. international congress of mechanical engineering. Ribeirão Preto, Brazil: 2013. p. 3468–79.
- [121] Lorenzini G, Lara MFE, Rocha LAO, Gomes MDN, Dos Santos ED, Isoldi LA. Constructal design applied to the study of the geometry and submergence of an oscillating water column. *Int J Heat Technol* 2015;33(2):31–8.
- [122] Elhanafi A, Fleming A, Macfarlane G, Leong Z. Underwater geometrical impact on the hydrodynamic performance of an offshore oscillating water column-wave energy converter. *Renew Energy* 2017;105:209–31.
- [123] Zheng S, Antonini A, Zhang Y, Greaves D, Miles J, Iglesias G. Wave power extraction from multiple oscillating water columns along a straight coast. *J Fluid Mech* 2019;878:445–80.
- [124] Falcão AF, Henriques JC, Cândido JJ. Dynamics and optimization of the OWC spar buoy wave energy converter. *Renew Energy* 2012;48:369–81.
- [125] Gomes RP, Henriques JC, Gato LM, Falcão AF. Hydrodynamic optimization of an axisymmetric floating oscillating water column for wave energy conversion. *Renew Energy* 2012;44:328–39.
- [126] Gradowski M, Gomes R, Alves M. Hydrodynamic optimisation of an axisymmetric floating oscillating water column type wave energy converter with an enlarged inner tube. *Renew Energy* 2020;162:61–72.
- [127] Portillo JC, Reis PF, Henriques JC, Gato LM, Falcão AF. Backward bent-duct buoy or forward bent-duct buoy? Review, assessment and optimisation. *Renew Sustain Energy Rev* 2019;112:353–68.
- [128] e Silva SR, Gomes R, Falcao A. Hydrodynamic optimization of the UGEN: Wave energy converter with U-shaped interior oscillating water column. *Int J Mar Energy* 2016;15:112–26.
- [129] Stansby P, Moreno EC, Stallard T. Capture width of the three-float multi-mode multi-resonance broadband wave energy line absorber M4 from laboratory studies with irregular waves of different spectral shape and directional spread. *J Ocean Eng Mar Energy* 2015;1(3):287–98.
- [130] Costello R, Teillant B, Weber J, Ringwood J. Techno-economic optimisation for wave energy converters. In: Proc. international conference on ocean energy. Dublin, Ireland: 2012. p. 1–5.
- [131] Wang L, Ringwood JV. Geometric optimization of a hinge-barge wave energy converter. In: Proc. European wave and tidal energy conference. Napoli, Italy: 2019.
- [132] Li Y, Peng H, Qiu W, Lundrigan B, Gardiner T. Hydrodynamic analysis and optimization of a hinged type wave energy converter. In: Proc. international conference on ocean, offshore and arctic engineering. Busan, Korea: 2016. p. 1–10.



- [133] Wu J, Yao Y, Li W, Zhou L, Götteman M. Optimizing the performance of solo Duck wave energy converter in tide. *Energies* 2017;10(3):1–19.
- [134] Kofoed JP. Optimization of overtopping ramps for utilization of wave energy. Tech. rep., Aalborg University; 2000.
- [135] Kofoed JP. Wave overtopping of marine structures: Utilization of wave energy [Ph.D. thesis], Aalborg University; 2002.
- [136] Victor L, Troch P, Kofoed JP. On the effects of geometry control on the performance of overtopping wave energy converters. *Energies* 2011;4(10):1574–600.
- [137] Martins JC, Goulart MM, Gomes MdN, Souza JA, Rocha LA, Isoldi LA, et al. Geometric evaluation of the main operational principle of an overtopping wave energy converter by means of construal design. *Renew Energy* 2018;118:727–41.
- [138] Fernandez H, Iglesias G, Carballo R, Castro A, Fraguela J, Taveira-Pinto F, et al. The new wave energy converter WaveCat: Concept and laboratory tests. *Mar Struct* 2012;29(1):58–70.
- [139] Fernandez H, Iglesias G, Carballo R, Castro A, Sánchez M, Taveira-Pinto F. Optimization of the WaveCat wave energy converter. *Coast Eng Proc* 2012;(33):5.
- [140] Allen J, Sampanis K, Wan J, Greaves D, Miles J, Iglesias G. Laboratory tests in the development of WaveCat. *Sustainability* 2016;8(12):1339.
- [141] Oliveira P, Taveira-Pinto F, Morais T, Rosa-Santos P. Experimental evaluation of the effect of wave focusing walls on the performance of the sea-wave slot-cone generator. *Energy Convers Manage* 2016;110:165–75.
- [142] Margheritini L, Stratigaki V, Troch P. Geometry optimization of an overtopping wave energy device implemented into the new breakwater of the hanstholm port expansion. In: Proc. international offshore and polar engineering conference. Rhodes, Greece: 2012. p. 1–8.
- [143] Vicinanza D, Margheritini L, Kofoed JP, Buccino M. The SSG wave energy converter: Performance, status and recent developments. *Energies* 2012;5(2):193–226.
- [144] Victor L. Optimization of the hydrodynamic performance of overtopping wave energy converters: Experimental study of optimal geometry and probability distribution of overtopping volumes [Ph.D. thesis], Ghent University; 2012.
- [145] Caska AJ, Finnigan TD. Hydrodynamic characteristics of a cylindrical bottom-pivoted wave energy absorber. *Ocean Eng* 2008;35(1):6–16.
- [146] Flocard F, Finnigan TD. Increasing power capture of a wave energy device by inertia adjustment. *Appl Ocean Res* 2012;34:126–34.
- [147] Kurniawan A, Moan T. Optimal geometries for wave absorbers oscillating about a fixed axis. *IEEE J Ocean Eng* 2012;38(1):117–30.
- [148] Zhao H, Sun Z, Hao C, Shen J. Numerical modeling on hydrodynamic performance of a bottom-hinged flap wave energy converter. *China Ocean Eng* 2013;27(1):73–86.
- [149] Renzi E, Leech J, Phillips I. WEC-GA optimisation tool for an oscillating wave surge converter. In: Proc. European wave and tidal energy conference. Cork, Ireland: 2017.
- [150] Hodge CW. Pitching paddles, hydraulic PTOs and shallow water waves: The development of a coupled non-linear modelling approach for WEC design [Ph.D. thesis], University of Edinburgh; 2020.
- [151] McCabe AP, Aggidis GA. A preliminary study into optimising the shape of a wave energy collector using a genetic algorithm. In: Proc. international conference on sustainable power generation and supply. Nanjing, China: 2009. p. 1–7.
- [152] McCabe AP. Constrained optimization of the shape of a wave energy collector by genetic algorithm. *Renew Energy* 2013;51:274–84.
- [153] McCabe A, Aggidis G, Widden M. Optimizing the shape of a surge-and-pitch wave energy collector using a genetic algorithm. *Renew Energy* 2010;35(12):2767–75.
- [154] Bódai T, Srinil N. Performance analysis and optimization of a box-hull wave energy converter concept. *Renew Energy* 2015;81:551–65.
- [155] Rodríguez CA, Rosa-Santos P, Taveira-Pinto F. Hydrodynamic optimization of the geometry of a sloped-motion wave energy converter. *Ocean Eng* 2020;199:107046.
- [156] Pecher A, Peter Kofoed J. Handbook of ocean wave energy. Springer Nature; 2017.
- [157] Pierson Jr WJ, Moskowitz L. A proposed spectral form for fully developed wind seas based on the similarity theory of SA Kitaigorodskii. *J Geophys Res* 1964;69(24):5181–90.
- [158] Hasselmann K, Barnett T, Bouws E, Carlson H, Cartwright D, Enke K, et al. Measurements of wind-wave growth and swell decay during the Joint North Sea Wave Project (JONSWAP). In: *Ergänzungsheft 8-12. Deutsches Hydrographisches Institut*; 1973.
- [159] Mérigaud A, Ringwood JV. Free-surface time-series generation for wave energy applications. *IEEE J Ocean Eng* 2017;43(1):19–35.
- [160] AMETS berth B wave buoy. 2020, <http://www.oceanenergyireland.ie/Observation>. [Accessed 10 September 2020].
- [161] Bozzi S, Archetti R, Passoni G. Wave electricity production in Italian offshore: A preliminary investigation. *Renew Energy* 2014;62:407–16.
- [162] Li Y, Yu Y-H. A synthesis of numerical methods for modeling wave energy converter-point absorbers. *Renew Sustain Energy Rev* 2012;16(6):4352–64.
- [163] Wendt F, Nielsen K, Yu Y-H, Bingham H, Eskilsson C, Kramer M, et al. Ocean energy systems wave energy modelling task: Modelling, verification and validation of wave energy converters. *J Mar Sci Eng* 2019;7(11):379.
- [164] Papillon L, Costello R, Ringwood JV. Boundary element and integral methods in potential flow theory: A review with a focus on wave energy applications. *J Ocean Eng Mar energy* 2020;6:303–37.
- [165] Folley M. Numerical modelling of wave energy converters: State-of-the-art techniques for single devices and arrays. Academic Press; 2016.
- [166] Bingham HB, Yu Y-H, Nielsen K, Tran TT, Kim K-H, Park S, et al. Ocean energy systems wave energy modeling task 10.4: Numerical modeling of a fixed oscillating water column. *Energies* 2021;14(6):1718.
- [167] Ransley E, Yan S, Brown S, Hann M, Graham D, Windt C, et al. A blind comparative study of focused wave interactions with floating structures (CCP-WSI Blind Test Series 3). *Int J Offshore Polar Eng* 2020;30(01):1–10.
- [168] Ruehl K, Michelen C, Kanner S, Lawson M, Yu Y-H. Preliminary verification and validation of WEC-Sim, an open-source wave energy converter design tool. In: International conference on offshore mechanics and arctic engineering, vol. 45547. American Society of Mechanical Engineers; 2014, p. V09BT09A040.
- [169] Bosma B, Lewis T, Brekken T, Von Joanne A. Wave tank testing and model validation of an autonomous wave energy converter. *Energies* 2015;8(8):8857–72.
- [170] DualSPHysics. 2020, <https://dual.sphysics.org/>. [Accessed 10 September 2020].
- [171] Zhu G, Graham D, Zheng S, Hughes J, Greaves D. Hydrodynamics of onshore oscillating water column devices: A numerical study using smoothed particle hydrodynamics. *Ocean Eng* 2020;218:108226.
- [172] Simonetti I, Cappiotti L, Elsafti H, Oumeraci H. Optimization of the geometry and the turbine induced damping for fixed detached and asymmetric OWC devices: A numerical study. *Energy* 2017;139:1197–209.
- [173] Hérault A, Bilotta G, Dalrymple RA. SPH on GPU with CUDA. *J Hydraul Res* 2010;48(S1):74–9.
- [174] Sheng W, Lewis A. Wave energy conversion of oscillating water column devices including air compressibility. *J Renew Sustain Energy* 2016;8(5):054501.
- [175] Falcão AF, Henriques JC. The spring-like air compressibility effect in oscillating-water-column wave energy converters: Review and analyses. *Renew Sustain Energy Rev* 2019;112:483–98.
- [176] López I, Carballo R, Taveira-Pinto F, Iglesias G. Sensitivity of OWC performance to air compressibility. *Renew Energy* 2020;145:1334–47.
- [177] Li A, Liu Y. New analytical solutions to water wave diffraction by vertical truncated cylinders. *Int J Nav Archit Ocean Eng* 2019;11(2):952–69.
- [178] Li A-j, Liu Y, Li H-j. New analytical solutions to water wave radiation by vertical truncated cylinders through multi-term Galerkin method. *Meccanica* 2019;54(3):429–50.
- [179] Penalba M, Kelly T, Ringwood J. Using NEMOH for modelling wave energy converters: A comparative study with WAMIT. In: Proc. European wave and tidal energy conference. Cork, Ireland: 2017.
- [180] Jin S, Patton RJ, Guo B. Viscosity effect on a point absorber wave energy converter hydrodynamics validated by simulation and experiment. *Renew Energy* 2018;129:500–12.
- [181] Cummins W. The impulse response function and ship motions. Tech. rep., David Taylor Model Basin Washington DC; 1962.
- [182] Morison JR, Johnson JW, Schaaf SA. The force exerted by surface waves on piles. *J Pet Technol* 1950;2(05):149–54.
- [183] Wang H, Sitanggang K, Falzarano J. Exploration of power take off in wave energy converters with two-body interaction. *Ocean Syst Eng* 2017;7:89–106.
- [184] Ji X, Al Shami E, Monty J, Wang X. Modelling of linear and non-linear two-body wave energy converters under regular and irregular wave conditions. *Renew Energy* 2020;147:487–501.
- [185] Wang R-q, Ning D-z. Dynamic analysis of wave action on an OWC wave energy converter under the influence of viscosity. *Renew Energy* 2020;150:578–88.
- [186] Penalba Retes M, Giorgi G, Ringwood JV. A review of non-linear approaches for wave energy converter modelling. In: Proc. European wave and tidal energy conference. Nantes, France: 2015. p. 1–10.
- [187] Penalba Retes M, Mérigaud A, Gilloteaux J-C, Ringwood J. Nonlinear Froude-Krylov force modelling for two heaving wave energy point absorbers. In: Proc. European wave and tidal energy conference. Nantes, France: 2015. p. 1–10.
- [188] Giorgi G, Ringwood JV. Computationally efficient nonlinear froude-Krylov force calculations for heaving axisymmetric wave energy point absorbers. *J Ocean Eng Mar Energy* 2017;3(1):21–33.
- [189] Giorgi G, Ringwood JV. Analytical representation of nonlinear froude-Krylov forces for 3-dof point absorbing wave energy devices. *Ocean Eng* 2018;164:749–59.
- [190] Merigaud A, Gilloteaux J-C, Ringwood JV. A nonlinear extension for linear boundary element methods in wave energy device modelling. In: Proc. international conference on offshore mechanics and arctic engineering. Rio de Janeiro, Brazil: American Society of Mechanical Engineers; 2012, p. 1–7.
- [191] Gudmestad OT, Moe G. Hydrodynamic coefficients for calculation of hydrodynamic loads on offshore truss structures. *Mar Struct* 1996;9(8):745–58.
- [192] Giorgi G, Ringwood J. Consistency of viscous drag identification tests for wave energy applications. In: Proc. European wave and tidal energy conference. Cork, Ireland: 2017. p. 1–8.

- [193] Guo B, Patton R, Jin S, Gilbert J, Parsons D. Nonlinear modeling and verification of a heaving point absorber for wave energy conversion. *IEEE Trans Sustain Energy* 2017;9(1):453–61.
- [194] Folley M, Whittaker T, Hoff JV. The design of small seabed-mounted bottom-hinged wave energy converters. In: Proc. European wave and tidal energy conference. Porto, Portugal: 2007. p. 1–10.
- [195] Giorgi G, Ringwood JV. Nonlinear froude-Krylov and viscous drag representations for wave energy converters in the computation/fidelity continuum. *Ocean Eng* 2017;141:164–75.
- [196] Sheng W, Alcorn R, Lewis T. Physical modelling of wave energy converters. *Ocean Eng* 2014;84:29–36.
- [197] Giorgi S, Davidson J, Jakobsen M, Kramer M, Ringwood JV. Identification of dynamic models for a wave energy converter from experimental data. *Ocean Eng* 2019;183:426–36.
- [198] Todalshaug JH, Åsgeirsson GS, Hjálmarsson E, Maillet J, Möller P, Pires P, et al. Tank testing of an inherently phase-controlled wave energy converter. *Int J Mar Energy* 2016;15:68–84.
- [199] Zhang X, Yang J. Power capture performance of an oscillating-body WEC with nonlinear snap through PTO systems in irregular waves. *Appl Ocean Res* 2015;52:261–73.
- [200] Nolan G, Ó Catháin M, Murtagh J, Ringwood J. Modelling and simulation of the power take-off system for a hinge-barge wave-energy converter. In: Proc. European wave energy conference. Cork: 2003.
- [201] Kurniawan A, Pedersen E, Moan T. Bond graph modelling of a wave energy conversion system with hydraulic power take-off. *Renew Energy* 2012;38(1):234–44.
- [202] Falcão AF, Henriques JC. Effect of non-ideal power take-off efficiency on performance of single-and two-body reactively controlled wave energy converters. *J Ocean Eng Mar Energy* 2015;1(3):273–86.
- [203] Li X, Chen C, Li Q, Xu L, Liang C, Ngo K, et al. A compact mechanical power take-off for wave energy converters: Design, analysis, and test verification. *Appl Energy* 2020;278:115459.
- [204] Cargo C, Hillis A, Plummer A. Strategies for active tuning of Wave Energy Converter hydraulic power take-off mechanisms. *Renew Energy* 2016;94:32–47.
- [205] Kim S-J, Koo W, Shin M-J. Numerical and experimental study on a hemispheric point-absorber-type wave energy converter with a hydraulic power take-off system. *Renew Energy* 2019;135:1260–9.
- [206] Henderson R. Design, simulation, and testing of a novel hydraulic power take-off system for the pelamis wave energy converter. *Renew Energy* 2006;31(2):271–83.
- [207] Falcão A, Gato L, Nunes E. A novel radial self-rectifying air turbine for use in wave energy converters. *Renew Energy* 2013;50:289–98.
- [208] Bacelli G, Genest R, Ringwood JV. Nonlinear control of flap-type wave energy converter with a non-ideal power take-off system. *Annu Rev Control* 2015;40:116–26.
- [209] Penalba M, Ringwood JV. A high-fidelity wave-to-wire model for wave energy converters. *Renew Energy* 2019;134:367–78.
- [210] Penalba M, Ringwood JV. Systematic complexity reduction of wave-to-wire models for wave energy system design. *Ocean Eng* 2020;217:107651.
- [211] Mérigaud A, Ringwood JV. A nonlinear frequency-domain approach for numerical simulation of wave energy converters. *IEEE Trans Sustain Energy* 2017;9(1):86–94.
- [212] Folley M, Whittaker T. Spectral modelling of wave energy converters. *Coast Eng* 2010;57(10):892–7.
- [213] Silva LS, Sergiienko NY, Pesce CP, Ding B, Cazzolato B, Morishita HM. Stochastic analysis of nonlinear wave energy converters via statistical linearization. *Appl Ocean Res* 2020;95:102023.
- [214] Yu Z, Faldes J. State-space modelling of a vertical cylinder in heave. *Appl Ocean Res* 1995;17(5):265–75.
- [215] Taghipour R, Perez T, Moan T. Hybrid frequency-time domain models for dynamic response analysis of marine structures. *Ocean Eng* 2008;35(7):685–705.
- [216] Pérez T, Fossen T. Time-vs. frequency-domain identification of parametric radiation force models for marine structures at zero speed. *Model Identif Control* 2008;29(1):1–19.
- [217] Perez T, Fossen TI. A matlab toolbox for parametric identification of radiation-force models of ships and offshore structures. *Model Identif Control* 2009;29(1):1–15.
- [218] Roessling A, Ringwood JV. Finite order approximations to radiation forces for wave energy applications. In: Proc. international conference on renewable energies offshore. Lison, Portugal: 2014. p. 359–66.
- [219] Faedo N, Peña-Sanchez Y, Ringwood JV. Finite-order hydrodynamic model determination for wave energy applications using moment-matching. *Ocean Eng* 2018;163:251–63.
- [220] Faedo N, Piuma FJD, Giorgi G, Ringwood JV. Nonlinear model reduction for wave energy systems: A moment-matching-based approach. *Nonlinear Dynam* 2020;102:1215–37.
- [221] Ljung L. System identification: Theory for the user. Upper Saddle River, NJ: PTR Prentice Hall; 1999.
- [222] Rao G, Unbehauen H. Identification of continuous-time systems. *IEE Proc, Control Theory Appl* 2006;153(2):185–220.
- [223] Ringwood J, Davidson J, Giorgi S. Identifying models using recorded data. In: Numerical modelling of wave energy converters. Elsevier; 2016. p. 123–47.
- [224] Ljung L. Perspectives on system identification. *Annu Rev Control* 2010;34(1):1–12.
- [225] Davidson J, Giorgi S, Ringwood JV. Linear parametric hydrodynamic models for ocean wave energy converters identified from numerical wave tank experiments. *Ocean Eng* 2015;103:31–9.
- [226] Giorgi S, Davidson J, Ringwood JV. Identification of wave energy device models from numerical wave tank data—Part 2: Data-based model determination. *IEEE Trans Sustain Energy* 2016;7(3):1020–7.
- [227] Davidson J, Giorgi S, Ringwood JV. Identification of wave energy device models from numerical wave tank data—Part 1: Numerical wave tank identification tests. *IEEE Trans Sustain Energy* 2016;7(3):1012–9.
- [228] Nguyen HN, Tona P. Wave excitation force estimation for wave energy converters of the point-absorber type. *IEEE Trans Control Syst Technol* 2017;26(6):2173–81.
- [229] Abdelrahman M, Patton R, Guo B, Lan J. Estimation of wave excitation force for wave energy converters. In: Proc. conference on control and fault-tolerant systems. Barcelona, Spain: IEEE; 2016. p. 654–9.
- [230] Guo B, Patton R, Jin S. Identification and validation of excitation force for a heaving point absorber wave energy converter. In: Proc. European wave and tidal energy conference. Cork, Ireland: 2017. p. 1–9.
- [231] Abdelkhalik O, Zou S, Robinett R, Bacelli G, Wilson D. Estimation of excitation forces for wave energy converters control using pressure measurements. *Internat J Control* 2017;90(8):1793–805.
- [232] Guo B, Patton RJ, Jin S, Lan J. Numerical and experimental studies of excitation force approximation for wave energy conversion. *Renew Energy* 2018;125:877–89.
- [233] Pena-Sanchez Y, Garcia-Abril M, Paparella F, Ringwood JV. Estimation and forecasting of excitation force for arrays of wave energy devices. *IEEE Trans Sustain Energy* 2018;9(4):1672–80.
- [234] Peña Y, Windt C, Davidson J, Ringwood JV. A critical comparison of excitation force estimators for wave-energy devices. *IEEE Trans Control Syst Technol* 2020;28(6):2263–75.
- [235] Giorgi S, Davidson J, Ringwood J. Identification of nonlinear excitation force kernels using numerical wave tank experiments. In: Proc. European wave and tidal energy conference. Nantes, France: European Wave and Tidal Energy Conference 2015; 2015. p. 1–10.
- [236] Penalba M, Ringwood JV. A review of wave-to-wire models for wave energy converters. *Energies* 2016;9(7):506.
- [237] Penalba M, Davidson J, Windt C, Ringwood JV. A high-fidelity wave-to-wire simulation platform for wave energy converters: Coupled numerical wave tank and power take-off models. *Appl Energy* 2018;226:655–69.
- [238] Penalba M, Ringwood JV. Linearisation-based nonlinearity measures for wave-to-wire models in wave energy. *Ocean Eng* 2019;171:496–504.
- [239] Davidson J, Windt C, Giorgi G, Genest R, Ringwood JV. Evaluation of energy maximising control systems for wave energy converters using OpenFOAM. In: Proc. OpenFOAM workshop. Guimarães, Portugal: 2019. p. 157–171.
- [240] Faldes J. Ocean waves and oscillating systems: Linear interactions including wave-energy extraction. Cambridge university press; 2002.
- [241] Fusco F, Ringwood JV. A simple and effective real-time controller for wave energy converters. *IEEE Trans Sustain Energy* 2012;4(1):21–30.
- [242] Davidson J, Genest R, Ringwood JV. Adaptive control of a wave energy converter. *IEEE Trans Sustain Energy* 2018;9(4):1588–95.
- [243] Babarit A, Clément AH. Optimal latching control of a wave energy device in regular and irregular waves. *Appl Ocean Res* 2006;28(2):77–91.
- [244] Nolan G, Ringwood J, Butler S, Leithead W. Optimal damping profiles for a heaving buoy wave energy converter. In: The 15th intl. offshore and polar engineering conf.. Seoul, Korea: 2005.
- [245] Clément A, Babarit A. Discrete control of resonant wave energy devices. *Phil Trans R Soc A* 2012;370(1959):288–314.
- [246] Sheng W, Lewis A. Power takeoff optimization for maximizing energy conversion of wave-activated bodies. *IEEE J Ocean Eng* 2016;41(3):529–40.
- [247] Bacelli G, Ringwood JV. A geometric tool for the analysis of position and force constraints in wave energy converters. *Ocean Eng* 2013;65:10–8.
- [248] Weber J, Costello R, Mouwen F, Ringwood J, Thomas G. Techno-economic WEC system optimisation - Methodology applied to Wavebob system definition. In: Proc. international conference on ocean energy. Bilbao, Spain: 2010. p. 1–5.
- [249] Teillant B, Costello R, Weber J, Ringwood J. Productivity and economic assessment of wave energy projects through operational simulations. *Renew Energy* 2012;48:220–30.
- [250] Chozas J. International levelised cost of energy for ocean energy technologies. Tech. rep., Ocean Energy System; 2015.
- [251] De Andres A, Medina-Lopez E, Crooks D, Roberts O, Jeffrey H. On the reversed LCOE calculation: Design constraints for wave energy commercialization. *Int J Mar Energy* 2017;18:88–108.
- [252] Dalton GJ, Alcorn R, Lewis T. Case study feasibility analysis of the Pelamis wave energy converter in Ireland, Portugal and North America. *Renew Energy* 2010;35(2):443–55.

- [253] Aubry J, Ruellan M, Ahmed HB, Multon B. Minimization of the kWh cost by optimization of an all-electric chain for the SEAREV Wave Energy Converter. In: Proc. international conference on ocean energy. Brest, France: 2008. p. 1–7.
- [254] De Andres A, Maillet J, Hals Todalshaug J, Möller P, Bould D, Jeffrey H. Techno-economic related metrics for a wave energy converters feasibility assessment. *Sustainability* 2016;8(11):1109.
- [255] Babarit A, Hals J, Muliawan MJ, Kurniawan A, Moan T, Krokstad J. Numerical benchmarking study of a selection of wave energy converters. *Renew energy* 2012;41:44–63.
- [256] Cordonnier J, Gorintin F, De Cagny A, Clément AH, Babarit A. SEAREV: Case study of the development of a wave energy converter. *Renew Energy* 2015;80:40–52.
- [257] Sirigu SA, Foglietta L, Giorgi G, Bonfanti M, Cervelli G, Bracco G, et al. Techno-economic optimisation for a wave energy converter via genetic algorithm. *J Mar Sci Eng* 2020;8(7):482.
- [258] Skinner SN, Zare-Behtash H. State-of-the-art in aerodynamic shape optimisation methods. *Appl Soft Comput* 2018;62:933–62.
- [259] Chong EK, Zak SH. An introduction to optimization. John Wiley & Sons; 2004.
- [260] Nocedal J, Wright S. Numerical optimization. Springer Science & Business Media; 2006.
- [261] Kachitvichyanukul V. Comparison of three evolutionary algorithms: GA, PSO, and DE. *Ind Eng Manag Syst* 2012;11(3):215–23.
- [262] Mitchell M. An introduction to genetic algorithms. MIT press; 1998.
- [263] Haupt RL, Ellen Haupt S. Practical genetic algorithms. Wiley Online Library; 2004.